



# Multi-modal and multi-subject modular organization of human brain networks

Maria Grazia Puxeddu<sup>a</sup>, Joshua Faskowitz<sup>a,c</sup>, Olaf Sporns<sup>a,b,c,d</sup>, Laura Astolfi<sup>e,f</sup>,  
Richard F. Betzel<sup>a,b,c,d,\*</sup>

<sup>a</sup> Department of Psychological and Brain Sciences, Indiana University, Bloomington, IN 47405

<sup>b</sup> Cognitive Science Program, Indiana University, Bloomington, IN 47405

<sup>c</sup> Program in Neuroscience, Indiana University, Bloomington, IN 47405

<sup>d</sup> Network Science Institute, Indiana University, Bloomington, IN 47405

<sup>e</sup> Department of Computer, Control and Management Engineering, University of Rome La Sapienza, Rome, 00185, Italy

<sup>f</sup> IRCCS, Fondazione Santa Lucia, Rome, 00142, Italy

## ABSTRACT

The human brain is a complex network of anatomically interconnected brain areas. Spontaneous neural activity is constrained by this architecture, giving rise to patterns of statistical dependencies between the activity of remote neural elements. The non-trivial relationship between structural and functional connectivity poses many unsolved challenges about cognition, disease, development, learning and aging. While numerous studies have focused on statistical relationships between edge weights in anatomical and functional networks, less is known about dependencies between their modules and communities. In this work, we investigate and characterize the relationship between anatomical and functional modular organization of the human brain, developing a novel multi-layer framework that expands the classical concept of multi-layer modularity. By simultaneously mapping anatomical and functional networks estimated from different subjects into communities, this approach allows us to carry out a multi-subject and multi-modal analysis of the brain's modular organization. Here, we investigate the relationship between anatomical and functional modules during resting state, finding unique and shared structures. The proposed framework constitutes a methodological advance in the context of multi-layer network analysis and paves the way to further investigate the relationship between structural and functional network organization in clinical cohorts, during cognitively demanding tasks, and in developmental or lifespan studies.

## 1. Introduction

The human connectome is the complete set of white-matter connections among neural populations (Hagmann et al., 2008; Sporns, 2011). This wiring diagram can be mapped and reconstructed using non-invasive imaging and represented as a graph or network (Bassett and Sporns, 2017). The connectome shapes pattern of neural activity, inducing correlations - functional connections - between remote neural elements (Fox et al., 2005; Friston, 1994; 2011). Human cognition and behavior are thought to be mediated by these distributed patterns of anatomical and functional connectivity among different brain areas (McIntosh, 2000; Mišić and Sporns, 2016).

The relationships between structural and functional connectivity is a central concept in network neuroscience, and linking brain function to its architecture is a long-standing goal in brain research (Honey et al., 2010; Park and Friston, 2013). A growing body of literature addresses this issue by trying to predict features of functional connectivity from structural features (Messé et al., 2015; Sarwar et al., 2021) (for a review see (Batista-García-Ramó and Fernández-Verdecia, 2018; Suárez et al., 2020) or (Bansal et al., 2018)). This has been done by implementing sta-

tistical (Mišić et al., 2016; Vázquez-Rodríguez et al., 2019) or communication (Crofts and Higham, 2009; Goñi et al., 2014; Zamani Esfahlani et al., 2022) frameworks, considering the coupling with biophysical dynamic systems (Adachi et al., 2012; Breakspear, 2017; Deco et al., 2009; Honey et al., 2007; Stam et al., 2016), or observing how brain lesions affect functional organization or link to behavior (Thiebaut de Schotten et al., 2020).

In addition to predicting one from another, structural and functional networks can be jointly analyzed to investigate common organizational properties, like modular structure, and see how they relate to each other. Modular organization is a hallmark of brain networks (Meunier et al., 2010; 2009; Sporns and Betzel, 2016) where groups of nodes are arranged into densely connected communities that support specialized cognitive function (Medaglia et al., 2015). This property has been observed in both anatomical and functional networks at different spatio-temporal scales (Betzel and Bassett, 2017). In fact, brain networks can be partitioned into communities in many different ways, resulting in either small modules, made of functionally specialized areas (Rosenthal et al., 2017), or large modules, hypothesized to support complex cognitive functions. A first contextual study (Betzel et al., 2013) mapped struc-

\* Corresponding author.

E-mail address: [rbetzel@indiana.edu](mailto:rbetzel@indiana.edu) (R.F. Betzel).

<https://doi.org/10.1016/j.neuroimage.2022.119673>.

Received 23 May 2022; Received in revised form 22 September 2022; Accepted 5 October 2022

Available online 17 October 2022.

1053-8119/© 2022 The Author(s). Published by Elsevier Inc. This is an open access article under the CC BY license (<http://creativecommons.org/licenses/by/4.0/>)

tural communities (defined in terms of random walks) to patterns of functional connectivity, suggesting that such communities model brain function. More recently, in (Diez et al., 2015), hierarchical modular structure has been investigated in group-average structural and functional networks, finding that there exist partitions that are highly modular in both types of connectivity. In (Fukushima et al., 2018), the overlap between structural and functional weights and modules has been investigated during different states of integration and segregation of time-varying functional networks, finding that structure and function are closer when functional connectivity presents an integrated network topology. However, a straightforward analysis of the interplay between anatomical and functional modules is missing.

In parallel, a growing number of studies have begun investigating multi-layer network models of brains (De Domenico, 2017; Vaiana and Muldoon, 2018). The multi-layer framework allows for multiple instances or observations of a networked system to be analyzed under a single model. In the context of brain network analysis, multi-layer network models can be constructed to capture the covariance structure of functional brain data (Bassett et al., 2011; Betzel et al., 2017; Braun et al., 2015; De Domenico et al., 2016; Puxeddu et al., 2020; Shine et al., 2016) or to establish node correspondence across networks representing different subjects' brains (Betzel et al., 2019).

In this work, we introduce a novel extension of the multi-layer framework to directly investigate the relationship between anatomical and functional modular organization, which also accounts for the multi-scale nature of modules and their subject specificity. This approach is conceived as an extension of the well-known, and widely employed, multi-layer modularity maximization model (Mucha et al., 2010). One of the greatest advantage of this model lies in its flexibility, and previous work demonstrated that one can easily modify its skeleton to address specific question of neuroscience (Zamani Esfahlani et al., 2021). Building on these works, we reformulate the coupling scheme of multi-layer modularity maximization. We incorporate a double inter-layer resolution parameter, one regulating the coupling between structural and functional connectivity matrices, and the other one regulating the inter-subject coupling. Thus, we simultaneously map communities across subjects and modes of connectivity, which enables direct comparison of multi-modal modules via community labels. We applied this model to MRI-derived anatomical and functional brain networks of healthy adults, to investigate how the modular structure of brain networks varies across subjects and connectivity modality. We describe which brain sub-systems form modules consistent across modalities and those that decouple from one another to form modality specific modules. In summary, our work extends the multi-layer modularity maximization framework and paves the way for future studies to investigate structure-function relationships in different contexts.

## 2. Methods

### 2.1. Experimental datasets and data processing

We leveraged anatomical and functional MRI data belonging to two independently acquired datasets that we describe below.

#### NKI dataset

First, we considered data from the Nathan Kline Institute Rockland Sample project (Nooner et al., 2012) (NKI-RS, [http://fcon\\_1000.projects.nitrc.org/indi/enhanced/](http://fcon_1000.projects.nitrc.org/indi/enhanced/)). Institutional Review Board approval was obtained for this project at the Nathan Kline Institute (#226781 and #239708) and at Montclair State University (#000983 A and #000983B) in accordance with relevant guidelines. All participants gave written informed consent or assent. The anonymized dataset is freely available at [http://fcon\\_1000.projects.nitrc.org/indi/enhanced/neurodata.html](http://fcon_1000.projects.nitrc.org/indi/enhanced/neurodata.html). The NKI dataset consists of imaging data from a community sample of subjects across a large portion of the human lifespan. We focused our analyses to subjects within the age

range of 20–40 years old, to concentrate on structure-function relationships without added influence of age-related changes. The data processing resulted in anatomical and functional networks made of 100 nodes from 123 subjects.

#### HCP dataset

We also analyzed data from the Human Connectome Project (HCP) (Van Essen et al., 2013), a consortium projected to construct a map of human brain circuits and their relationship to behavior in a large population of healthy adults. The study was approved by the Washington University Institutional Review Board and informed consent was obtained from all subjects. It comprises a large cohort of subjects (>1000), from which multiple imaging data were acquired (diffusion MRI, resting-fMRI, task-fMRI and MEG/EEG), together with behavioral and genetic data. Details of the image acquisition and minimal preprocessing can be found in (Glasser et al., 2013). We focused only on the 100 unrelated subjects. Of the 100 subjects, 5 have been excluded after preprocessing. This resulted in obtaining structural and functional networks of 95 subjects (56% female, mean age =  $29.29 \pm 3.66$ , age range = 22–36). The processing of the data was made with the same cortical parcellation used for NKI data, which led to structural and functional networks made of 100 nodes.

#### Transformation of anatomical networks into correlation networks

One important consideration to keep in mind when pursuing analysis on structure-function relationships, is that these two types of networks have differing interpretations and different topology. Anatomical networks embody physical pathways linking distinct brain regions. Their weights represent white-matter fiber tracts and are all non-negative. Moreover, while their density might vary based on the dimension of brain regions (i.e., parcellation adopted in the data processing) or reconstruction procedure, generally they are sparse. On the contrary, functional networks encode statistical relationships between the activity recorded from distinct brain regions. In our case they measure the correlation of BOLD activity between two brain areas, resulting in fully connected networks with either positive and negative weights.

The different architecture of anatomical and functional networks might hamper topological analysis aimed at investigating their relationship, biasing the results. For this reason, after the reconstruction of anatomical brain networks, we converted these sparse matrices into structural correlation matrices by computing the Pearson's correlation between each pair of rows, as in (Amico and Goñi, 2018). In this way, the anatomical edge weights were restricted to the interval  $[-1, 1]$  and the structural matrices were comparable to the functional ones. This is desirable in light of the construction of the multi-modal multi-layer network.

Note that SC and FC are two different objects and in principle one can transform any of the two to accommodate the topology of the other. We intentionally manipulated the SC matrices in agreement with the state-of-the-art literature on structure-function relationship, where biophysical, communication or statistical models operate on structural connectivity to find correlations with functional connectivity (Suárez et al., 2020).

#### Multi-modal modularity optimization through traditional multi-layer models

The main objective of this work was to study the relationship between functional and structural connectivity from the perspective of their shared and unique modular structure. For this sake, one possibility is to recover communities of the brain networks through community detection (Fortunato, 2010), employing an algorithm based on modularity optimization. Modularity ( $Q$ ) (Girvan and Newman, 2002; Newman, 2012; Newman and Girvan, 2004) is a global quality function that estimates how strongly communities are internally connected with respect to a chance level, so that optimizing  $Q$  results in the detection of assortative communities, i.e. groups of nodes that are internally dense and

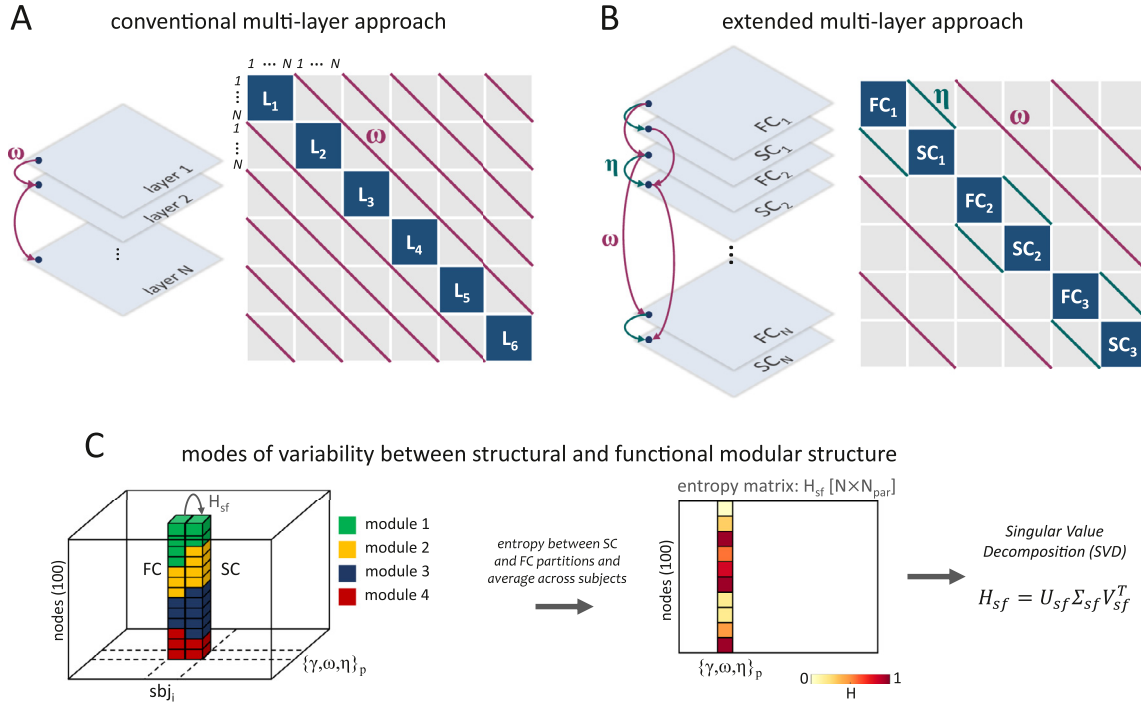


**Fig. 1. Schematic representation of the extended multi-layer modularity optimization.** (a) Conventional approach. Single-layer networks are aligned over the main diagonal of a square matrix of dimension [number of nodes  $\times$  number of layers]. Modules are found by optimizing the modularity function on this network in which each node is connected to itself across layers through the resolution parameter  $\omega$ . (b) Extended approach. Functional and structural connectivity matrices of each subjects are aligned over the diagonal of a square matrix sized [number of nodes  $\times$  number of subjects  $\times$  2 (type of connectivity)]. Modularity optimization is run on this network, considering each node connected to itself within modality and across subjects through  $\omega$ , and between type of connectivity through  $\eta$ . (c) Schematic representation of the methods used to investigate the relationship between structural and functional modular structure. For each subject and point in the parameter space identified by  $\gamma$  (spatial resolution parameter),  $\omega$  and  $\eta$ , we obtain a partition of structural and functional networks into modules (left), on which we can compute the nodal entropy. By averaging across subjects we obtain an entropy matrix  $H_{sf}$  of dimension  $N \times N_{par}$  (nodes  $\times$  combinations of parameters) (right) that we can decompose into principal components to identify recurrent structural-functional relationships in the parameter space.

externally sparse.  $Q$  is defined as follows:

$$Q(\gamma) = \sum_{ij} [W_{ij} - \gamma P_{ij}] \delta(\sigma_i, \sigma_j). \quad (1)$$

where  $W_{ij}$  and  $P_{ij}$  are the actual and expected weights of the link connecting nodes  $i$  and  $j$ . The variable  $\sigma_i \in \{1, K\}$  indicates to which cluster node  $i$  belongs, and  $\delta(x, y)$  is equal to 1 if  $x = y$  and 0 otherwise. The parameter  $\gamma$  represents a spatial resolution weight that scales the influence of the null model, affecting the number and size of modules recovered. Using high  $\gamma$  values results in many small communities and vice-versa.

A multi-layer version of  $Q$  has been introduced to detect communities in multi-layer networks (Mucha et al., 2010), where layers correspond to estimates of the same network at different points in time, individuals, or connection modalities. The multi-layer analog of  $Q$  is defined as:

$$Q(\gamma, \omega) = \sum_{ijrt} [(W_{ijr} - \gamma P_{ijr}) \delta_{rt} + \omega \delta_{ij}] \delta(\sigma_{ir}, \sigma_{jt}). \quad (2)$$

Nodes are linked to themselves across layers through the resolution parameter  $\omega$  (Fig. 1a). Its value affects the homogeneity of communities across layers (indicated through  $r$  and  $t$ ), in a way that small  $\omega$  values emphasize layer-specific modular structure, while big  $\omega$  values point out communities shared across layers (Puxeddu et al., 2019). The optimization of  $Q(\gamma, \omega)$  returns, for each layer, a partition of the network into assortative communities, whose dimensions and consistency across layers depend on two parameters of spatial and a cross-layers resolution. Applying multi-layer modularity optimization, instead of the single-layer one to each network, is generally convenient; the multi-layer approach is more resistant to noise (Puxeddu et al., 2021a) and returns commu-

nity labels that are coherent across layers, so that one can easily track their evolution.

Historically, applications of this method have been, almost exclusively, to time-varying estimates of functional connectivity (Bassett et al., 2011; Betzel et al., 2017; Braun et al., 2015). However, this multi-layer approach can be also used to link structural and functional modular organization. Multiple single-subject SC and FC matrices from the NKI can be averaged across subjects to form group representative networks. These, in turn, can be concatenated in a two-layers modularity matrix of dimension  $N \times Modalities$  (number of nodes  $\times$  connection modality:  $100 \times 2$ ) on which modularity optimization can be iterated with different combination of  $\gamma$  and  $\omega$ . In this case,  $\gamma$  would impact the dimension of the communities, while  $\omega$  their homogeneity between SC and FC.

## 2.2. Multi-modal and multi-subject modularity optimization

In this work, we propose an extension of multi-layer modularity framework, formulated in order to handle information about different subjects and connection modality (SC or FC) simultaneously. Specifically, we allow the inter-layer coupling parameter  $\omega$  introduced in Eq. 2 to adopt different values when linking subjects and modality. Thus, we could assume that, in addition to the spatial resolution parameter  $\gamma$ , we simultaneously consider two inter-layer resolution parameters,  $\omega$  and  $\eta$ , that couple each node  $i$  with itself across subjects (indicated with  $r$  and  $t$ ) and modalities (indicated with  $f$  and  $s$ ) respectively. A schematic of this coupling scheme is reported in Fig. 1b, while its expression is

reported in Eq. 3:

$$Q(\gamma, \omega, \eta) = \sum_{ijfsrt} [(W_{ijfr} - \gamma P_{ijfr})\delta_{rt}\delta_{fs} + \dots \omega\delta_{ij}\delta_{fs} + \eta\delta_{ij}(1 - \delta_{fs})]\delta(\sigma_{irf}, \sigma_{jts}). \quad (3)$$

Here,  $\omega$ , which we refer to as the *subject resolution parameter*, controls the homogeneity of the communities across all the participants, while  $\eta$ , the *modality resolution parameter*, regulates the coupling of the partitions between FC and SC networks within each participant. The  $\eta$  parameter operates in a way similar to  $\omega$ , so that for increasing  $\eta$  values we obtain structural and functional partitions that are increasingly coupled. Thus, setting low  $\eta$  values would lead to partitions that highlight features that are unique to structure and function, while larger  $\eta$  values would correspond to features that are shared.

We built a multi-layer network as shown in Fig. 1b, aligning along the main diagonal anatomical and functional modularity matrices of the 123 healthy adult subjects from the NKI dataset. We obtained a square matrix of dimension  $NS \times N \times M$  (number of subjects  $\times$  number of nodes  $\times$  connection modality:  $123 \times 100 \times 2 = 24600$ ). By optimizing  $Q(\gamma, \omega, \eta)$  we partitioned nodes in single networks (the individual layers) into modules. We ran the modularity optimization varying the three resolution parameters in the range  $[s_{\min}, 1]$ , with  $s_{\min} = 2.12 \times 10^{-6}$  indicating the minimum weight of the SC matrices. In this range we considered 50 equally distanced values, so that we obtained an ensemble of 125,000 partitions ( $50 \times 50 \times 50$ ) for each subject and type of connectivity. We ran the optimization employing the openly-available genlouvain package (<http://netwiki.amath.unc.edu/GenLouvain/GenLouvain>), implemented in Matlab (Jutla et al., 2011). As in the classic multi-layer version, the algorithm returns as an output a partition of each network-layer into modules. These partitions are encoded as vectors of dimension  $N$ , where each entry represents the allegiance of node  $i$  to module  $k$ . Thus, in our extended model, for each combination of the resolution parameters  $\{\gamma, \omega, \eta\}$  we obtained  $NS \times M$  partitions under the form of  $N$ -dimensional vectors. A schematic of this output is reported in Fig. 1(c).

When running multi-layer modularity, the choice of the null model  $P_{ijrf}$  is crucial. There exist many possible definitions of null models, and we adopt the approach to set  $P_{ijrf} = 1$  for all  $i, j, s, f$ . This is referred to as *uniform null model*, and it has been shown to be a good model to deal with correlation matrices (Bazzi et al., 2016; Traag et al., 2011), resulting in communities with well-known topographic features. Since functional networks are rendered as temporal correlation matrices, and we converted anatomical networks into structural correlation matrices, we could use the uniform null model in all the network's layers. As for the parameter  $\omega$ , instead, it can be considered in two configurations: (i) all-to-all, meaning that nodes are linked to themselves through  $\omega$  across all the layers (used if layers represent categorical variables); (ii) temporal, connecting nodes only between consecutive layers (used in time-varying networks). In this case, layers connected through  $\omega$  represent different subjects, so that we used the first configuration.

Lastly, we want to emphasize that the transformation applied to SC networks is fundamental for this analysis and in general for those analysis aimed at comparing SC and FC topological organization. If we had preserved SC networks in the form of a sparse positive matrix with weights possibly much higher than 1 (i.e., maximum weight reachable in FC networks), the community detection process would have been biased: depending it on the weights of the matrices, it would have found modules reflecting almost exclusively the anatomical modular organization. Moreover, this transformation allowed us to use the same mathematical instruments (i.e., the same spatial null model in the optimization) on both matrices.

### Analysis of the communities

#### Preliminary statistics on the communities

Through the multi-layer modularity maximization, we obtained a joint partition of anatomical and functional brain networks into nodal

modules for each subject and for each combination of the resolution parameters. A widespread and easy approach is to focus on specific and fixed values of resolution parameters. Instead, we explored solutions over a range of parameters values, seconding the multi-scale organization of the brain networks (Betzel and Bassett, 2017). Specifically, we assessed the modular structure by tuning the resolution parameters in the range  $[s_{\min}, 1]$  sampled with 50 values, obtaining 125,000 partitions of the multi-layer networks for every subject's SC and FC matrix. This corresponds to an ensemble of 250,000 partitions for each subject ( $125,000 \times 2$ ). Within this broad set of solutions, however, we restricted further investigation to a narrower subset, focusing on parameter combinations that result non-trivial partitions. Criteria for selection included:

1. Number of clusters ( $NC$ ). We considered partitions with a number of modules falling in the range  $[5, 20]$ . Given that  $N=100$ , these modules will be made of 20 to 5 nodes on average. This choice allowed us for a multi-scale analysis where we explored a large portion of the spatial resolution spectrum, from very fine to coarse partitions, while automatically rejecting trivial ones, like singleton partitions (i.e. partitions made of 1 node), or 2-modules partitions (which merely partition the hemispheres). We excluded combinations of resolution parameters that produced both structural and functional partitions with an average number of modules outside this range.
2. Variability among subjects. We discarded partitions in which either functional or structural community structure was identical across all the subjects, as many studies demonstrate that the patterns of brain connectivity are subject-specific. We quantified the variability among subjects of node's assignment through the normalized community entropy:

$$h_i = -\frac{1}{\log_2(K)} \sum_{k=1}^K p_i(k) \log_2(p_i(k)). \quad (4)$$

where  $k$  indicates the communities, and  $p_i(k)$  is the fraction of subjects in which node  $i$  belong to community  $k$ . By dividing for  $\log_2(K)$  we normalized this measure in the range  $[0, 1]$ , with 0 indicating identical assignments and 1 maximal variability. By averaging  $h_i$  for all the nodes, we obtained  $H = \frac{1}{N} \sum_{i=1}^N h_i$ , a measure of the variability of the entire partition across subjects, within each type of connectivity. We ignored resolution parameters providing  $H = 0$  across subjects.

Based on these criteria, we considered  $N_{par} = 3732$  combinations of  $\{\gamma, \omega, \eta\}$  (out of the total 125,000), in the ranges  $\gamma \in [0.02, 0.4]$ ,  $\omega \in [2.12 \times 10^{-6}, 0.16]$ ,  $\eta \in [2.12 \times 10^{-6}, 1]$ . We based all the following analysis on this sample of partitions.

#### Modes of variability across modality and across subjects

In order to analyze the variability of communities across acquisition modalities, we computed the community entropy (Eq. 4) between structural and functional partitions, which returns the variability of each nodes assignment to a module in the two modalities. The precise entropy values depend on the specific combination of the resolution parameters  $\{\gamma, \omega, \eta\}$ . Through Principal Component Analysis (PCA) we aimed to inspect the parameter space and see if there existed patterns of variability that are recurrent inside this space. Thus, for each point in the parameter space (identified by different combinations of  $\{\gamma, \omega, \eta\}$ ), we computed the entropy between partitions coming from functional and structural networks, and we averaged this value across subjects. We aligned the resulting vectors in a matrix  $H_{sf}$  of dimension  $N \times N_{par}$ , and we subjected it to Singular Value Decomposition (SVD). SVD decomposes the matrix  $H_{sf}$  into singular vectors  $U_{sf} \in [N \times N]$  and  $V_{sf} \in [N_{par} \times N]$ , and singular values  $\Sigma_{sf} \in [N_{par} \times N]$ , so that:

$$H_{sf} = U_{sf} \Sigma_{sf} V_{sf}^T. \quad (5)$$

The matrices  $U_{sf}$  and  $V_{sf}$  are orthonormal by definition and contain the principal component scores and coefficients, respectively. The columns of  $U_{sf}$  can be interpreted as the modes of variability between SC and



FC partitions, while the values in the rows in  $V_{sf}$  indicate where these modes are likely to appear in the parameter space. The diagonal elements of  $\Sigma_{sf}$  contain the information about the covariance with which each component explains the variability across SC and FC. These passages have been outlined in Fig. 1(c).

Limiting the study to the components explaining most of the variance between SC-FC community entropy, we identified the points in the parameter space where these components are most strongly expressed. In this way, we divided the parameter space into non-overlapping regions that correspond to distinct patterns of coupling between structural and functional modules. Within each one of these regions we extracted representative partitions for both structural and functional networks, by computing the Variation of Information (VI) (Meil, 2007), an information theoretic measure of distance between pairs of partitions, and recorded the centroid, the partition least distant from all other partitions (i.e. with lowest VI). A schematic representation of this analysis can be found in Supplementary Material, Figure S2.

We performed a similar analysis to identify modes of variability across subjects, focusing our analyses on inter-subject variation of anatomical or functional modules, independently. We built a matrix  $H_{sbj}$  of dimension  $N \times N_{rep}$  containing in each column the vector of the entropy  $h$  computed among subjects within modality each modality (structural/functional connectivity). We executed the SVD to decompose  $H_{sbj}$  in the singular vectors  $U_{sbj} \in [N \times N]$  and  $V_{sbj} \in [N_{par} \times N]$ , and singular values  $\Sigma_{sbj} \in [N_{par} \times N]$ :

$$H_{sbj} = U_{sbj} \Sigma_{sbj} V_{sbj}^T. \quad (6)$$

We did this for both structural and functional partitions. Again, the matrices  $U_{sbj}$  and  $V_{sbj}$  are orthonormal and contain the principal component scores and coefficients. Here, we interpret the columns of  $U_{sbj}$  as the modes of variability of the partitions across subjects. The values in the rows in  $V_{sbj}$  indicate where these modes are likely to appear in the parameters space, while the diagonal elements of  $\Sigma_{sbj}$  contain the variance with which each component explains the variability across subjects.

### 3. Results

The brain's modular structure reveals groups of brain regions that are functionally or anatomically related. Identifying this architecture at different scales can lead to important clinical and behavioral insights. In this work, we introduced an extension of the multi-layer modularity framework, developed to analyze multi-subject multi-modal datasets. By concatenating structural and functional connectivity matrices of different subjects and treating them as coupled layers of a multi-layer network, our approach is meant to simultaneously map brain communities into subjects and type of connectivity at different scales. Then, the communities obtained in such a way will be analyzed with standard indices, like variation of information (VI) and entropy (H), to assess their similarity across modality and/or subjects. We will also present a PCA analysis meant to identify scales in which the structure-function relationship has a stable pattern.

In the following sections, we illustrate the results of the application of our new framework to anatomical and functional networks obtained from healthy adult subjects of the NKI dataset. We will first comment on the results in light of the traditional multi-layer framework and then, as a validation, we will replicate the analysis on an independent dataset.

#### 3.1. Multi-modal modular structure with conventional multi-layer modularity optimization

As a first step, we show how topological properties of anatomical and functional networks can be linked through the conventional multi-layer modularity optimization framework (Fig. 1a). To this end, we extracted representative anatomical and functional group-averaged networks for

the NKI dataset by averaging SC and FC matrices across the 123 subjects. Hence, we built a two-layers modularity matrix and we iterated the conventional multi-layer modularity optimization (Eq. 2) 100 times with combinations of  $\gamma$  and  $\omega$  whose values span the range  $[s_{min}, 1]$ . For each combination of  $\gamma$  and  $\omega$ , the algorithm returned a partition of the two group-averaged networks into modules. Then, we retained only non-trivial partitions with non-singleton communities, which led to consider  $\gamma$  in the range  $[s_{min}, 0.83]$ . Here, we comment how the two resolution parameters affect the optimization's output in terms of coupling between anatomical and functional modules and how we can study their relationship at different scales.

By computing the cross-layer VI and nodal entropy (that are the VI and entropy between FC and SC partitions), and averaging across the 100 iterations, we show how the resolution parameter  $\omega$  controls the homogeneity of modules across layers, and thus, in our case, connection modalities. These indices measure how much nodes' assignments to a community vary at the node level (entropy) and globally (VI). As expected, entropy values decreased monotonically with  $\omega$  (Fig. 2(a)), which means that higher  $\omega$ -values leads to high coupling between FC and SC partitions. Analogously, VI decreased monotonically with  $\omega$  (Fig. 2(b), blue line), meaning that also globally FC and SC partitions tend to get closer one another, until  $\omega > 0.7$ , at which point the partitions are identical ( $VI = 0$ ,  $H_{sf} = 0$ ). Thus, by tuning  $\omega$  in its range, we were able to explore different levels of structure-function relationships, highlighting modular configurations that are distinctive of the connection modality, or shared between them.

By definition,  $\gamma$  affects the size of the detected communities. However, in Fig. 2(a), one can see how  $\gamma$ -values also impact the cross-layer homogeneity, in a proportional way (even if to lesser extent with respect to  $\omega$ , as shown by the marginal plots). This is trivially explained by the progressive diminishing of the dimension of the modules. In fact, any two partitions with a number of clusters close to the number of nodes are intuitively more similar. Also the lowest  $\gamma$ -values brought to more coupled partitions, and for a similar reason (few bigger clusters are more likely to comprehend the same nodes). Further statistics and plots regarding the effect of the spatial resolution parameter on the dimension of the discovered communities have been reported in Supplementary Material, Figure S4.

Focusing on a specific  $\gamma$ -value ( $\gamma = 0.16$ ), we reported in Fig. 2(d) an example of how modules in SC and FC networks gradually reconfigure, increasing  $\omega$ , to meet a higher overlap. The most evident change, by eye, happens in the areas covering the primary motor cortex. These belong to hemispheric-specific clusters in the SC partitions for low  $\omega$  (as expected, since structural connectivity favors short-distance connections), but then increasing  $\omega$  they start participating in the same modules, as in FC partitions. Unpacking the nodal entropy we could better observe these local properties. For instance, for every brain system we can keep track of the entropy across  $\omega$  (Fig. 2(c)) and see at which rate they reconfigure. If we average across  $\omega$  then (Fig. 2(e)), we could have an estimate of how likely different brain system change their modules assignment to increase the overlap between structural and functional partitions. For instance, we found that ventral attention network present high entropy until  $\omega = 0.7$  (where FC and SC partitions become identical), while visual and temporal areas participate in modules that are overlapped in SC and FC partitions even before  $\omega = 0.7$ . Note that in Fig. 2(c,d) we showed modular structure and nodal entropy up to  $\omega = 0.7$ . We excluded the possibility of a perfect alignment between structural and functional modular organization, given the different nature of the signals and the fact that structural modules underpin a static wiring of anatomical pathways, while functional modules are shaped by dynamic statistical relationships between brain areas.

In summary, we showed how conventional multi-layer modularity optimization can be used to investigate the coupling between structural and functional topological properties. However, applied in this manner, this approach can only operate on averaged brain network data, ignoring single-subject's information. Indeed, this model is able to track commu-

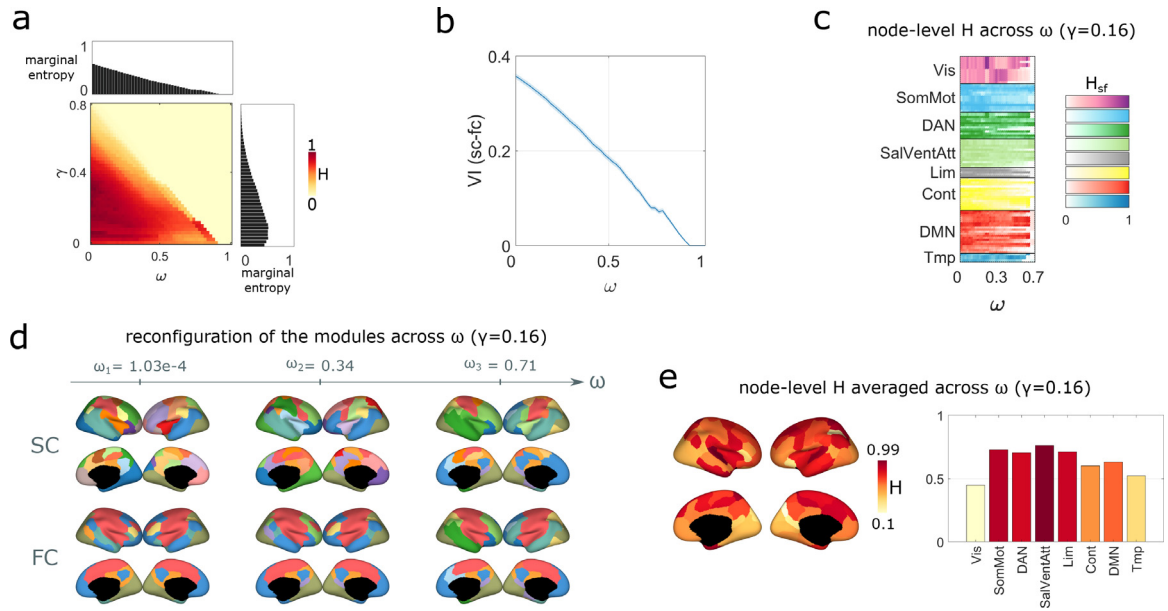


**Fig. 2. Conventional multi-layer modularity optimization to couple structural and functional communities in the group-average networks.** (a) Entropy between structural and functional partitions varying the resolution parameters  $\omega$  and  $\gamma$ . (b) Variation of Information (VI) between SC and FC partitions across  $\omega$ . (c) Node's entropy between SC and FC partitions in the  $\omega$ -range ( $\gamma = 0.16$ ). (d) Projection on the brain cortex of the structural and functional partitions obtained with multi-layer modularity optimization with  $\gamma = 0.16$  and increasing the inter-layer coupling parameter  $\omega$ . The different communities are rendered through a color code. (e) Entropy between FC and SC partitions ( $\gamma = 0.16$ ) averaged across  $\omega$  projected in the brain surface.

nities along only one dimension, which we can choose to be time (e.g. as in (Bassett et al., 2011)), subjects (e.g. as in (Betzel et al., 2019)), or connection modality (as shown here). In the next section we illustrate how the extension that we propose overcomes this limit. For sake of clarity, note that in the just presented conventional multi-layer framework the parameter  $\omega$  couples SC and FC networks. In our extension instead, SC and FC will be linked by a new parameter  $\eta$ , while  $\omega$  will bridge matrices across subjects. This is well explicated in Methods, Eq. 2 and Eq. 3.

### 3.2. Detection of multi-subject multi-modal modular structure

In the previous section we illustrated how the multi-layer framework could be applied to multi-modal network data, focusing on group-averaged networks. Here, we show how the extended multi-layer modularity optimization (Eq. 3) can detect modules in structural and functional networks simultaneously from the 123 subjects of the NKI dataset. The modularity optimization over our extended model in fact returned a partition of each network layer into modules. For each combination of  $\{\gamma, \omega, \eta\}$  and subject we obtained both the anatomical and functional modular structure encoded in N-dimensional vectors that associate nodes to labeled modules. This time, the output of the optimization algorithm depends on three resolution parameters  $\{\gamma, \omega, \eta\}$ , that we varied in the range  $[s_{\min}, 1]$ . One challenge is that some of the parameters will yield uninformative partitions. We illustrate how we excluded unwanted partitions and, once restricted the space of investigation, how  $\{\gamma, \omega, \eta\}$ -values affect the number of modules and their coupling across subjects and connection modality.

To retain only informative partitions, we studied how the spatial and cross-subject resolution parameters,  $\gamma$  and  $\omega$ , impact the statistics of the communities and we restricted their range consequently. According to our formulation of the multi-layer framework, the spatial resolution parameter,  $\gamma$ , influences the number of communities, while  $\omega$  impacts the homogeneity of the partitions across subjects. Here, we computed the optimization while tuning the parameters in the range  $[s_{\min}, 1]$ , and we observed how the number of clusters and community entropy are distributed in the parameter space. Results are reported in the Supplementary Material, Figure S3. As expected, we found that setting  $\gamma$  to

high (low) values leads to many small (few big) clusters, while increasing  $\omega$  leads to lower variability of the modular structure across subjects (Figure S3(f-i)). We selected non-singleton partitions with 5–20 communities, where nodes' assignment to the communities differs for at least one subject (i.e. entropy within modality greater than 0). This procedure narrowed the  $\gamma$  and  $\omega$  ranges down, into a non-rectangular parameter space limited by  $\gamma \in [0.02, 0.4]$ ,  $\omega \in [2.12 \times 10^{-6}, 0.16]$ , where anatomical and functional partitions are respectively made of  $NC_s = 16 \pm 9.8$  and  $NC_f = 8 \pm 4.8$  clusters. Each combination of the parameters in this sub-space corresponds to an informative partition. As a demonstration, we computed the distance of all the partitions from a set of canonical brain systems (Thomas Yeo et al., 2011), also referred to as intrinsic connectivity networks (ICNs), observing that the minimum distance falls in the selected subspace (see Supplementary Material, Figure S5).

Once we identified a sub-space of meaningful partitions through the parameters  $\gamma$  and  $\omega$ , we could observe how the  $\eta$  parameter enables to explore different levels of coupling between structural and functional modular structure. In our model,  $\eta$  determines the extent to which identified communities persist across types of connectivity (note that in the conventional case presented in the previous section this role was covered by  $\omega$ ). The hypothesis is that there would be significant differences among structural and functional partitions when the coupling parameter is low, but the partitions would converge increasing  $\eta$ 's value. To test this hypothesis we computed the VI between structural and functional partitions for each  $\eta$ -value, averaging in the restricted  $\{\gamma, \omega\}$  ranges. The results, reported in Fig. 3(d), showed a decreasing trend of VI for increasing  $\eta$ -values (blue line). Low  $\eta$ -values yield weak coupling between FC and SC partitions, while high  $\eta$ -values yield strong coupling between the same partitions. This supports the hypothesis that the brain modular structure differs between types of connectivity, but that adjusting  $\eta$  we can encourage the algorithm to find features that are unique to function and structure, as well as shared features. Note that this is analogous to what we found using the connection modality as layer-dimension in the group-averaged conventional model (Fig. 2(b)). The only difference is the range of VI-values, which is shifted down in the conventional case. This might be an effect of the group-average, that leads to flatten network's properties over the sample.

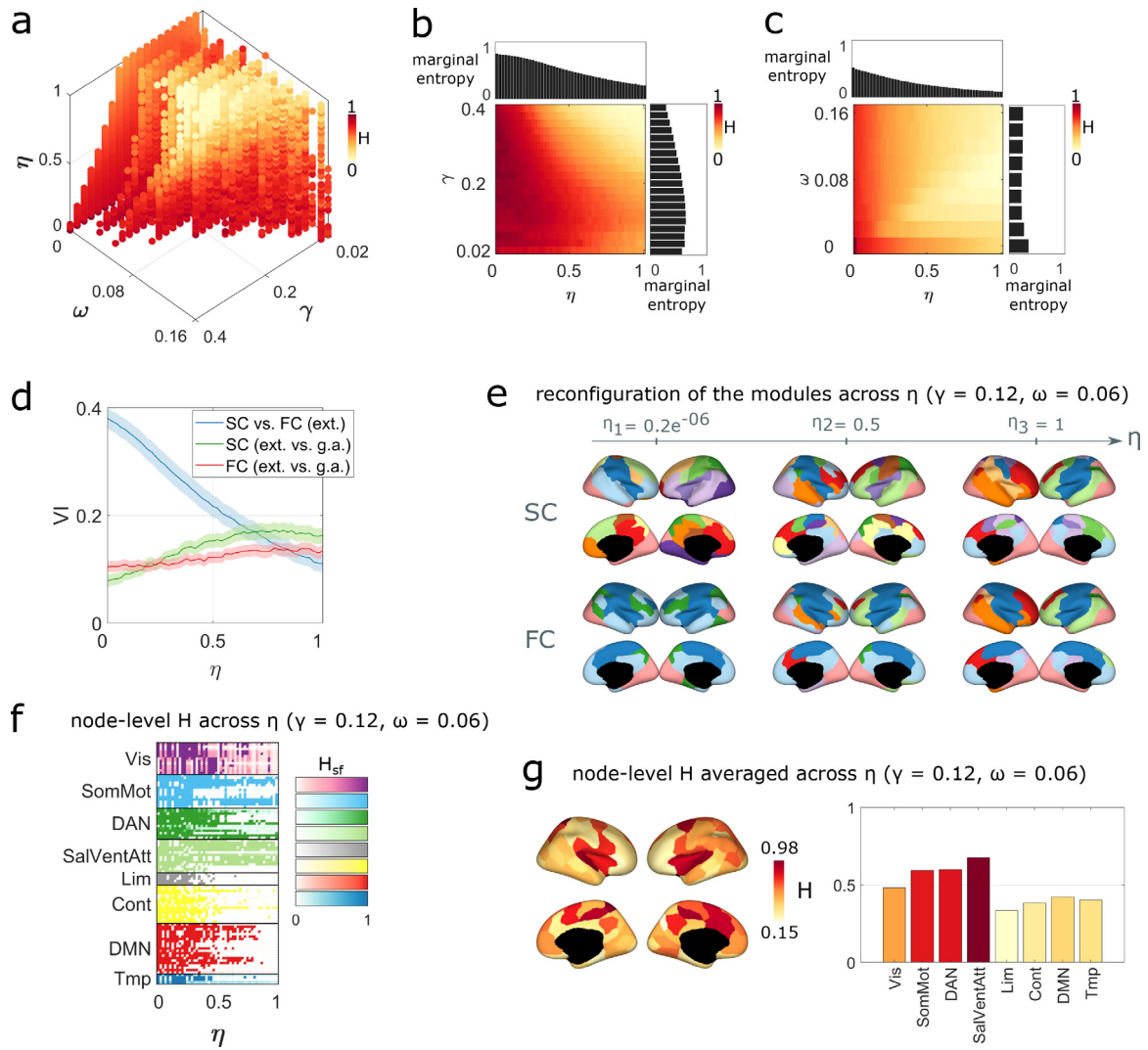


**Fig. 3. Extended multi-layer modularity optimization to couple structural and functional communities in multi-subject datasets.** (a) Entropy between structural and functional partitions varying the three resolution parameters  $\{\gamma, \omega, \eta\}$  projected in the parameter space (averaged across subjects). (b) Projection of the entropy in the 2-dimensional space constituted by  $\eta$  and  $\gamma$  (average across  $\omega$ ). (c) Projection of the entropy in the 2-dimensional space constituted by  $\eta$  and  $\omega$  (average across  $\gamma$ ). (d) Distance between SC and FC partitions across the  $\eta$ -range (blue line) in terms of Variation of Information, having averaged across  $\gamma$  and  $\omega$ ; mean (dark line) and confidence interval (shaded area) are shown. The red and green plots report the distance between functional and structural partitions obtained with this extended model and those in the group-average analysis. (e) Projection on the brain cortex of the consensus partitions obtained with the extended multi-layer modularity optimization for increasing  $\eta$  ( $\gamma = 0.12$ ;  $\omega = 0.06$ ). Different communities are rendered through a color code. (f) Node-wise entropy between SC and FC partitions (averaged across subjects) in the  $\eta$ -range ( $\gamma = 0.12$ ;  $\omega = 0.06$ ), and its average projected on the brain surface (g).

Furthermore, in Fig. 3(d), we showed the VI computed between the partitions obtained with the new model and those from the previous group-average case (green and red lines). In this case the VI tends to increase with  $\eta$ , meaning that the higher  $\eta$  is, the more that the multi-layer partitions diverge from the traditional ones. However, these VI-values remain low ( $< 0.2$ ) along the  $\eta$ -range, so that increasing  $\eta$  affects the coupling between SC and FC partition to a greater extent in the new framework, than the divergence of such partitions with the traditional ones.

The parameters  $\gamma$  and  $\omega$ , are responsible for modulating the number of clusters and homogeneity of the partitions across subjects (Figure S3). We showed that the coupling between structural and functional modules is analogously governed by  $\eta$ . A further demonstration of this is in Fig. 3(a-c), where we reported the normalized nodal entropy ( $H$ ) between SC and FC partitions, first calculated within subjects and then averaged across all subjects, in the restricted parameter space. As expected, we found that  $H$  varies monotonically only with  $\eta$ , decreasing

when such parameter increases. Overall, we observed that  $H$  varies all over the parameter space and it shows its lowest values, meaning high coupling between FC and SC partitions, when all the parameters  $\{\gamma, \omega, \eta\}$  are set to high values.

Our multi-subject and multi-modal modularity is meant to detect modules of different sizes and more or less consistent across subjects and types of connectivity. However, in some cases, instead of observing how global properties of the modules vary across the whole parameter space, one may want to investigate a more focused set of partitions and provide a more detailed description of the community structure. Our algorithm allows for this possibility. For instance, in Fig. 3(e-g), we isolated the structural and functional partitions obtained with  $\gamma = 0.12$  (meaning on average  $NC_s = 13.9 \pm 1.7$  and  $NC_f = 7.3 \pm 1.9$ ) and  $\omega = 0.06$  (ensuring good consistency across subjects). We observed how in this specific case the partitions become progressively coupled across  $\eta$  (Fig. 3(e)). To further explore structure-function relationship, we can also look at which brain systems are more prone to participate in similar communities in



SC and FC networks for increasing  $\eta$ -values, and which instead remain modality-specific, as we did in the previous section (Fig. 3(f)). In the subspace defined by  $\{\gamma = 0.12, \omega = 0.06\}$  - arbitrarily chosen - we observed that the DMN together with the temporal, limbic and control systems belong to the first category, while the somato-motor area, DAN and salience and ventral attention networks belong to the second one (Fig. 3(g)). The same analysis can be used to explore communities at coarser or finer scales, meaning focusing on lower or higher  $\gamma$ -values (see Figure S6). Furthermore, in a similar way, one can also explore how either structural or functional modular organization reconfigures across subjects (see Figure S10).

Here, we have illustrated the community structure that can be obtained using multi-layer multi-modal modularity maximization. Its output depends on three resolution parameters whose value impacts modules size as well as variability across subjects and connection modality. Predefined heuristic about the output community structure allowed us to focus on parameter ranges where the character of detected communities is consistent with previous reports, while still capturing meaningful inter-subject and inter-modality variability. We also showed how our model allows for the coupling between structural and functional partitions to be systematically adjusted. A more detailed description of the modular structure in the parameter space will follow.

### 3.3. Modes of variability between connection modalities

In the previous section we identified a subset of parameters where partitions could be considered meaningful for imaging-based analyses. Inside this subspace, we showed in which way the three resolution parameters  $\{\gamma, \omega, \eta\}$  affect the scale of the partitions and the magnitude of their variability between types of connectivity and among subjects. Now, we want to discover if there exist recurrent patterns of inter-modality variability which are encoded in the parameters subspace in a non-random manner. In fact, knowing how the SC-FC coupling depends on the scales of the communities is important in more pragmatic studies,

for instance in clinical-oriented studies, where we might want to amplify individual-specific features of the SC-FC relations (for example to find correlations with a clinical index), or features of such relations that are shared across a cohort. For this purpose, we stored in a  $100 \times 3732$  ( $N \times N_{par}$ ) matrix the vectors containing the normalized nodal entropy across modalities (one vector for each point in the sub-sampled parameter space) and we performed the Principal Component Analysis (PCA) on this matrix. Through the PCA we obtained 99 principal component scores (in the form of orthonormal vectors of length equal to the number of nodes), and the relative coefficients, informative of their contribution on each of the 3732 rows of the data. Thus, we identified the modes of variability projecting the scores and the coefficients on the cortex surface and on the parameter space, respectively.

In Fig. 4 we reported the results relative to the first five components, that, out of the 99, explain most of the variance of the SC-FC community coupling (12.53%, 9.67%, 7.77%, 6.17%, 5.69% respectively), while the remaining components each explains less than 5% of the variance (see Supplementary Figure S7).

Globally the first five  $PC_s$  occupied different zones in the three-dimensional parameter space (Fig. 4(a-e)).  $PC_1$  was expressed at high  $\eta$  and  $\gamma$  values, corresponding to a subspace in which inter-modality variability was low and the brain is partitioned into fine modular structure, i.e. many small modules. Projecting  $PC_1$  scores onto the cortex showed that, in this region of the parameter space, the nodes whose module's assignment differs most between FC and SC networks belong to the Dorsal Attention Network (DAN), the Salience and Ventral Attention Network and the somatosensory and motor areas (Fig. 4(f,k)). On the contrary, other regions like those from the Control, Default Mode Network (DMN), Limbic, and Temporal systems, showed higher consistency between the two connectivity measures within this subspace. The other principal components were expressed in other regions of the parameters space and showed different patterns of inter-modality variability, suggesting that patterns of variability of the SC and FC modular structure were resolution-dependent. For example,  $PC_2$  coefficients as-

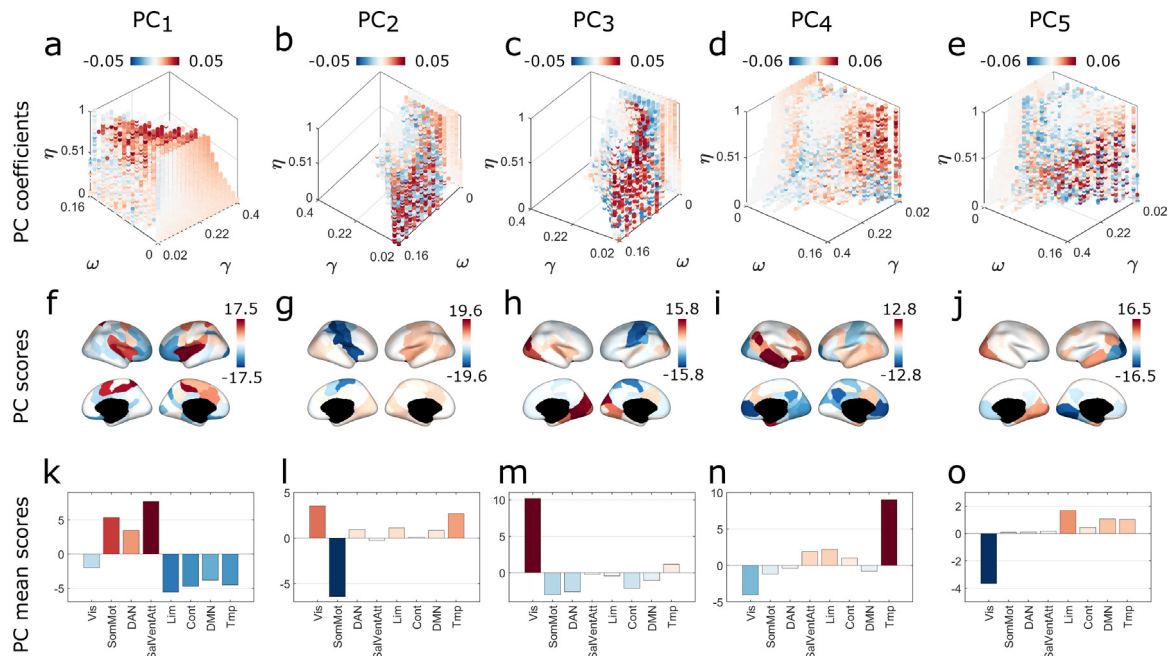


**Fig. 4.** Principal component analysis (PCA) for the detection of modes of variability between structural and functional community structure. Columns of this figure correspond to the first five components of the decomposition. (a-e): projection of the first five PC coefficients into the parameter space identified by the parameters  $\gamma, \omega, \eta$ . (f-j): projection on the cortex surface of the first five PC scores. (k-o): average within the functional systems of the first five PC scores. In each component, brain areas colored with red present community assignment highly variable between functional and structural networks. These variations mostly occur in the space of parameter identified by red dots. Blue-colored brain areas instead, identify stable node's community assignment in the relative blue points of the parameter space.



summed high positive values in the subspace where  $\gamma$  and  $\eta$  are low and  $\omega$  is high, corresponding to networks parsed in few clusters, highly coupled across subjects and barely coupled between connection modality. Here, the regions whose module assignments were more variable between FC and SC networks are those involved in the visual and temporal systems. The regions belonging to the somatosensory and motor systems instead, show higher consistency between modalities. In  $PC_4$  coefficient are more expressed at low  $\gamma$ , and high  $\omega$  and  $\eta$ , that is where partitions present few clusters, high correspondence among subjects and a good level of overlap between modalities. In this subspace the visual and somatomotor systems, together with the DAN and DMN, tend to maintain the same modules allegiance in SC and FC networks, while the regions mostly located in the temporal area are more likely to change module passing from SC to FC networks.

We hypothesized that these modes of entropy are non-randomly structured in the parameter space, but rather, they are robust to different choices that one must make in the building of a multi-modal network. To prove that, we replicated an identical analysis on three differently built multi-layer networks. In the first, we considered a finer parcellation of the brain, made of 200 nodes. In the second, we run our extended multi-layer framework on the structural and functional networks from only one hemisphere (the left one). We perform this analysis to evaluate the role of inter-hemispheric connections, which are generally stronger in functional networks while more difficult to reconstruct in anatomical networks. In the last one, we built the multi-layer network transform-

ing the SC matrices through the Spearman correlation, instead of the Pearson correlation. While by using the Pearson correlation we already addressed the main topological concerns (i.e., weight range and sparsity), a non linear type of correlation, like the Spearman's, might better handle other properties of the SC networks, like for instance the exponential distribution of the weights. Statistically comparing the results of the PCA, we observed that, in all the cases, there is a significant correlation between the principal components scores of the different models, which suggests that structure-function relationships are encoded in the parameter space in a non-random fashion. These validations are reported in section 10 of Supplementary Material.

Once identified well-structured modes of entropy between structural and functional modular organization, one could ask how this large amount of data could be treated. One solution we suggest in this section is performing a consensus analysis within the sub-regions of the parameter space identified by the principal components. Thus, a deeper analysis of the first five Principal Component is presented in Fig. 5. First, we reported in the parameter space, through different colors, the 100 points corresponding to the right tail ( $\approx 2.5\%$  of the values) of  $PC$  coefficients, in order to better pinpoint the regions where the  $PC$  were most expressed (Fig. 5(a)). Then, for each component, we only considered the partitions corresponding to these points, to investigate which brain areas show the highest variability in the modules' allegiance between anatomical and functional networks, and across subjects (Fig. 5(b,c)). Moreover, for each set of partitions corresponding to the five  $PC$ , we

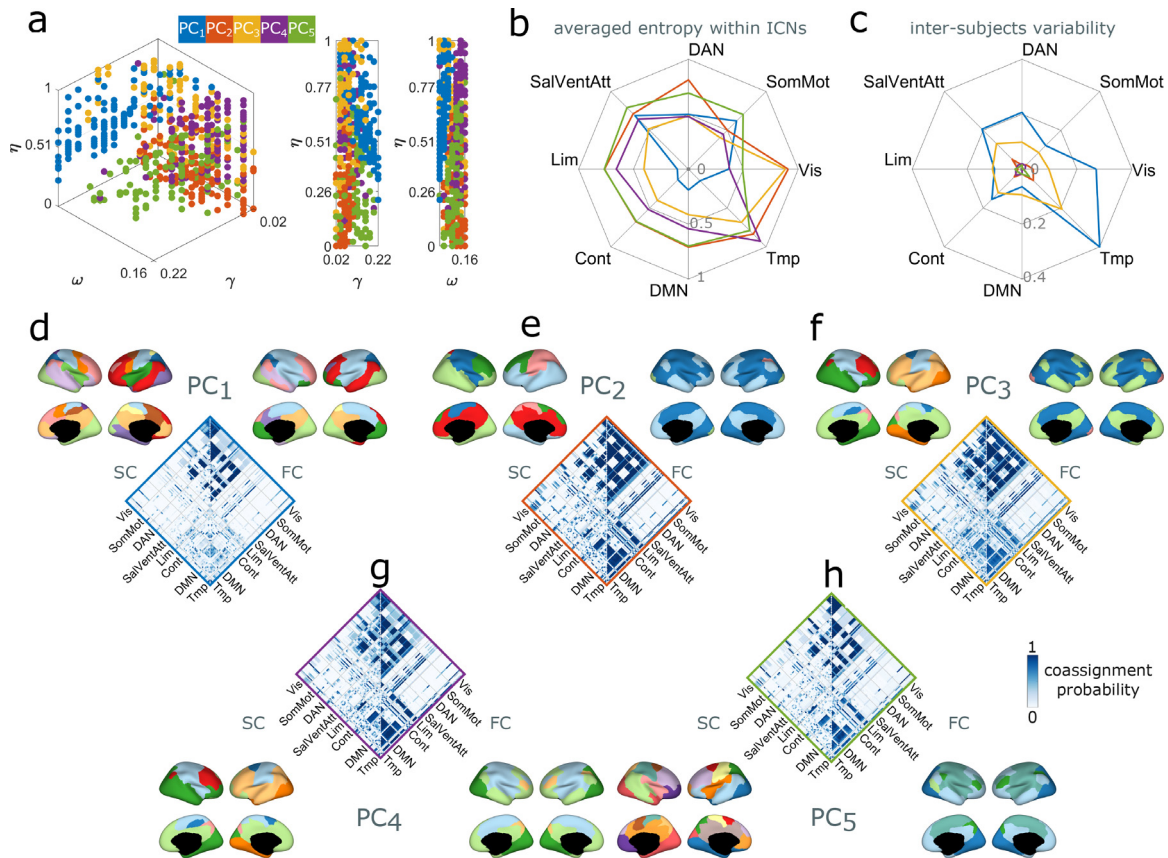


**Fig. 5. Modes of variability and representative partitions.** (a) Projection on the parameter space of the 100 points, corresponding to different combinations of  $\gamma$ ,  $\omega$ ,  $\eta$ , where the first five components are more expressed. Components are identified through color code. For each component we computed the community entropy between the 100 SC and FC partitions identified in panel (a). By averaging these values across subjects and within functional systems (b) we obtained information about the nodes whose assignment varies most within each component ( $std \in [0.02, 0.35]$ ). Instead, by averaging across combinations of  $\{\gamma, \omega, \eta\}$  of each of the five subspace (c) we gained information about the variability of node's assignment across subjects, for each component ( $std \in [0.02, 0.26]$ ). These results have been reported through spider plots. (d-h) For each component we selected the partitions corresponding to the points highlighted in panel (a) and we computed a representative partition among them, for both structural and functional networks, and the agreement matrix (co-assignment probability of each pair of nodes).

also reported the agreement matrix and a representative partition for both structural and functional networks (Fig. 5(d-h)). The agreement matrix shows the probability that each pair of nodes belongs in the same module in the subspace identified by  $PC_5$ .  $PC_5$  were mostly expressed in different zones of the parameter space and for each of them we could observe different values of community entropy within the ICNs or across subjects, as well as different agreement matrices and representative partitions. For instance, as we intuited before,  $PC_1$  was mostly expressed at low  $\omega$ , and mid-range  $\gamma$  and  $\eta$ . The partitions falling in this subspace presented a good overlap between structural and functional connectivity. The brain regions whose module's assignment was most variable belong to the ventral attention network, the DAN and part of the somatomotor area, which, as one can observe in the representative partitions, were joined together in the functional partition, while remaining separated in the structural one. On the contrary, the highest level of inter-subject variability is observed in the brain areas underlying temporal nodes. Similar observations, with different conclusions, can be done for the other four components.

An analogous PCA analysis has been conducted to evaluate modes of variability of the modular structure across subjects, in both cases of structural and functional connectivity, and it has been reported in the Supplementary Material (Figures S8 and dummyTXdummy-S9).

Taken together, these results suggest the existence of inter-modality variability patterns that are well structured in the parameter space. The way sub-systems are coupled between structural and functional connectivity highly depends on the choice of the  $\gamma$ ,  $\omega$ ,  $\eta$ -values. In other words, the same functional or cognitive system could participate in the same modules in functional and structural networks, or not, according to the topological scale of the partitions (tuned through  $\gamma$ ) or their consistency

across subjects (modulated by  $\omega$ ). This information is crucial and has to be borne in mind by a potential user, above all in contexts where structure-function relationships are linked to clinical or behavioral measures of the human brain. Such relationships would be dependent on the choice of  $\gamma$ ,  $\omega$  and  $\eta$ , which in turn are set arbitrarily by the user.

#### 3.4. Detecting multi-modal multi-subject modular structure in the Human Connectome Project dataset

In order to validate the results of the study, we reproduced the analysis on a subset of the Human Connectome Project dataset (Van Essen et al., 2013). It comprises anatomical and functional connectivity data from 95 unrelated healthy adult subjects.

After having built a multi-subject multi-modal network as in Fig. 1b, we ran multi-layer modularity optimization. Then, in order to assess patterns of inter-modality variability, we performed PCA on the entropy matrices obtained computing the node's entropy between structural and functional partitions in each point of the parameter space given by  $\gamma$ ,  $\omega$ ,  $\eta$ . We reported in Fig. 6(a-e) the projection on the brain surface of the first three principal component's coefficients, which explained most of the variance of the variability across modality ([12.99, 7.78, 5.73]% respectively).

The PCA analysis executed on the NKI and HCP datasets led to comparable results in terms of patterns of entropy between connection modality. To prove it, we looked for statistical correlations between the scores of the first principal components of the two datasets. Results are reported in Fig. 6(d-g). We found that the first components of the two datasets,  $NKI_{PC_1}$  and  $HCP_{PC_1}$ , are positively correlated ( $pval = 0.03$ ,  $r = 0.21$ ). For both datasets, in the subspace defined by

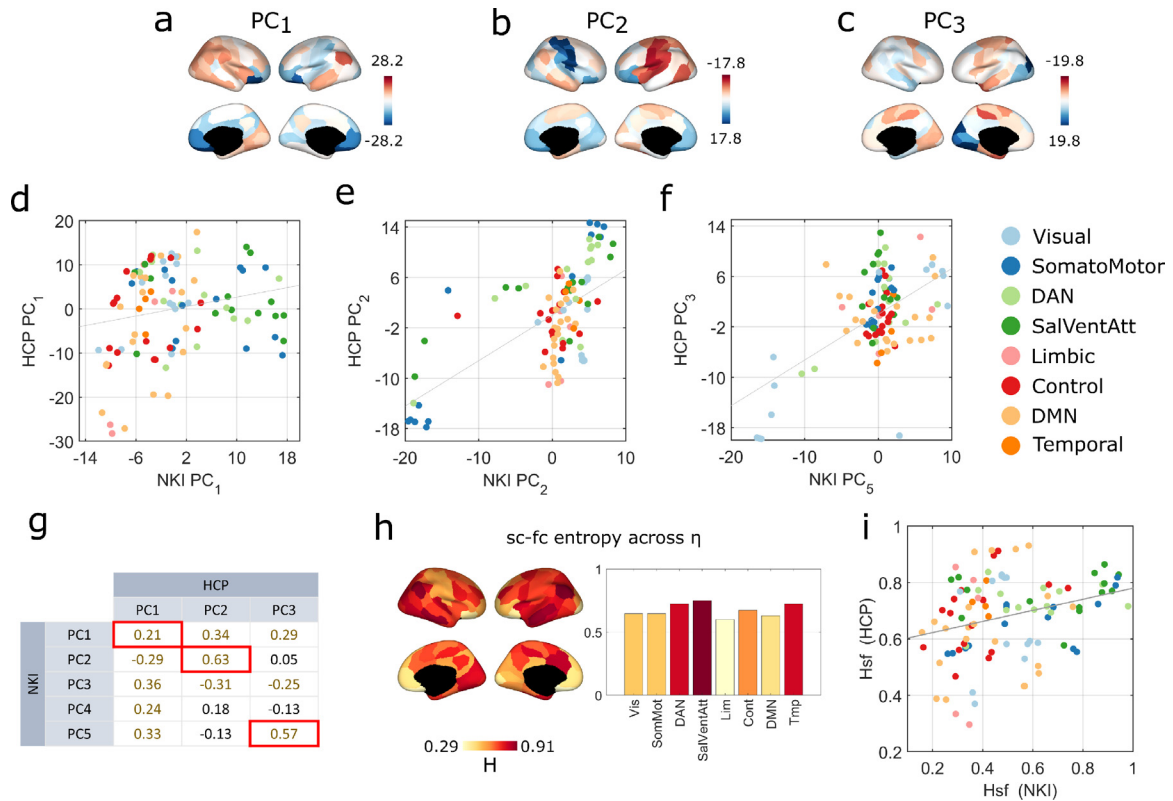


**Fig. 6. Analysis of the Human Connectome Project dataset.** (a-c) Representation on the brain cortex of the coefficients of the first three components generated from the PCA analysis performed on the HCP dataset. These components broadly correspond to those of the NKI dataset, as shown through the correlation maps reported in panels (d-f). (g) Tables reporting correlation coefficients for each pair of components. the pairs that we represented in panels (d-f) are bounded in red. Correlation coefficients non statistically significant have been reported in black. p-values have been corrected for multiple comparisons. (h) Entropy between FC and SC partitions of the HCP averaged across  $\eta$  ( $\gamma = 0.10$ ;  $\omega = 0.02$ ) and projected on the brain surface. This is the equivalent to Fig. 3(g) for the HCP dataset. At this scale, the obtained values of entropy across modalities are correlated across the two different datasets ( $r = 0.3$ ,  $pval = 0.003$ ) (i).

these components, the brain regions whose modules assignment differs most between structural and functional connectivity belonged to the DAN, the Salience and Ventral Attention networks, and the somatomotor area. At the same time, the DMN together with the Control Network and Temporal areas pertain to modules shared with SC and FC matrices. Note that we have already commented on this for the NKI networks in Fig. 4(k). Here we are demonstrating the robustness of the results by validating them on an independent dataset. Other significant correlations, even stronger, have been found between:  $NKI_{PC_2}$  and  $HCP_{PC_2}$  ( $pval < 10^{-3}$ ,  $r = 0.63$ );  $NKI_{PC_5}$  and  $HCP_{PC_5}$  ( $pval < 10^{-3}$ ,  $r = 0.57$ ). These three correlations have been proven significant also with a non parametric spin test (Alexander-Bloch et al., 2018), with which we obtained p-values equal to [0.0198, 0.0002, 0.0008], respectively.

We further illustrated the consistency of results across independent datasets by focusing on the inter-modality variability at one specific scale (see Fig. 6(j,k)). We selected the partitions corresponding to  $\{\gamma = 0.12, \omega = 0.06\}$  for the NKI, and  $\{\gamma = 0.10, \omega = 0.2\}$ . Here, we observed low inter-subject variability and 7 modules for the functional partitions ( $CNf_{NKI} = 7 \pm 1.9$ ,  $CNf_{HCP} = 6 \pm 0.9$ ) and 10 for the structural ones ( $CNs_{NKI} = 13 \pm 1.7$ ,  $CNs_{HCP} = 7 \pm 0.6$ ). At this scale, the system-averaged values of inter-modality variability significantly correlated in the two datasets ( $r = 0.3$ ,  $pval = 0.003$ ).

We replicated the analysis on a second dataset, the HCP, independently acquired, but similar in terms of participants' number and age. The reported findings corroborated the results that we first obtained with the NKI dataset. Indeed, modes of inter-modality variability appeared to be robust across datasets and confirmed the multi-scale organization of the human brain networks.

#### 4. Discussion

In this work, we explored how the modular structure of the human brain networks is organized across structural and functional connectivity metrics. While most of the literature focuses on the comparison and prediction at the nodes and edge weights level (Suárez et al., 2020), we investigated structure-function relationship at the mesoscale level. In doing this we proposed a novel multi-modal framework, developed on top of the widely-used multi-layer modular optimization (Mucha et al., 2010), where structural and functional connectivity matrices are stacked and linked by three resolution parameters  $\{\gamma, \omega, \eta\}$ . Through this extension we detected the modules of the human brain networks across structural and functional connectivity and among subjects, simultaneously. The three resolution parameters represent a lens through which we could investigate the modular structure of the brain networks, zooming in and out towards organizational traits that are unique or shared among connectivity modalities or subjects. Thus, we explored how modules are configured across spatial scales and at different levels of coupling of the nodes across subjects and types of connectivity.

##### 4.1. Relationships between structural and functional modular structure across subjects

The principal aim of this work was to characterize the community organization of brain networks across types of connectivity. Our results suggest that there is not a single way to describe the overlap between structural and functional modular organization. Rather, we observed that this overlap depends on the spatial resolution of modules (controlled by the parameter  $\gamma$ ), but also on the inter-subject and inter-modality resolution (regulated by the parameters  $\omega$  and  $\eta$ , respectively). Trivially, the strength of the inter-modality resolution ( $\eta$ ) was proportional to the overlap between structural and functional modules. As for the dependence on the spatial resolution ( $\gamma$ ), previous studies have shown how brain networks display a multi-scale community organization (Betzel and Bassett, 2017). Therefore it is intuitive that the relationship of this organization between different types of connectivity

will also be multi-scale. Specifically, we observed a higher SC-FC modular coupling in finer partitions. Tuning the cross-subject resolution ( $\omega$ ) instead, we found a higher coupling between structural and functional partitions when considering low community variability across subjects.

In this study, we presented criteria to narrow the parameter space to the maximum possible number of combinations of parameters that yield to non-trivial solutions, and analyzed the structure-function relationship within this large space. Future investigations, however, might be focused on a narrower subspace from the beginning, basing on the research question or hypothesis. For instance, one might want to highlight group-level features of the network organization and focus only on high  $\omega$ , or vice versa on low  $\omega$  to identify subject-specific attributes (for example in clinical studies where the aim is usually to find relations with subject-level clinical outcomes).

Through principal component analysis we divided the parameter space into regions where we identified modes of variability between anatomical and functional modules. We described in detail the structure-function relationship explained by the first five components, expressing most of the variance in the PCA. In this way, we went from observing 3732 sets of structural and functional partitions, to the analysis of five recurrent cases. These first five components are located in the parameter space as follows:  $PC_1$  high- $\eta$ , low- $\omega$ , high- $\gamma$ ;  $PC_2$  low- $\eta$ , low-to-high- $\omega$ , low- $\gamma$ ;  $PC_3$  low- $\gamma$ , low- $\omega$ , high- $\eta$ ;  $PC_4$  high- $\eta$ , high- $\omega$ , low- $\gamma$ ;  $PC_5$  high- $\gamma$ , high- $\omega$ , low- $\eta$ . These results confirmed that the structure-function coupling, at the modular level, is mediated by the topological scale. In the best possible condition from the SC-FC coupling point of view, represented by  $PC_1$ , the regions whose community assignment varies the most between modality are mainly associated to the ventral attention network. Interestingly, this might align with results in (Vázquez-Rodríguez et al., 2019), where the coupling between structural and functional connectivity in this area has shown to be statistically lower than chance when compared to a null model. The DMN instead, is the functional system where the relationship between structure and function is more heterogeneous, as for some components we observed a coupled modular organization, while for some other components we did not. This could be due to the high number of circuits in which DMN participates and the variable dynamics it exhibits (Buckner and DiNicola, 2019; Vatansever et al., 2015; Zhang et al., 2016). In  $PC_2$ , high entropy values between structural and functional communities are widespread in the cortex, involving all the ICNs except for the somatosensory system. This result fits recent studies where structural and functional connectivity was found to be more consistent in the unimodal (sensory) cortex with respect to transmodal cortex (Paquola et al., 2019; Preti and Van De Ville, 2019). A possible interpretation for the general high-entropy in  $PC_2$  could be linked to the fact that it is expressed at low- $\omega$ , where partitions are variable across subjects. As functional brain networks have been shown to be subject-specific (Finn et al., 2015; Gordon et al., 2017; Laumann et al., 2015), so will be their relationship with the underlying structural network. Thus, when the coupling among subjects is low (low- $\omega$ ), it is reasonable to expect a high variability between structural and functional partitions over different brain regions.

All these findings suggest that the relationship between anatomical and functional modular organization is not well summarized by a single spatial or temporal scale. Different studies have been carried out focusing on a single-scale community structure and its relationship with cognitive output, providing important insight into brain functions. However, our work, together with (Betzel and Bassett, 2017; Betzel et al., 2019), suggests that multi-scale analyses are needed to gain a more comprehensive understanding of the relation between brain structure, function, and cognition. It is worth specifying that, while we tackled and analyzed the multi-scale set of structural and functional partitions through a PCA, there exist also other methods with which we can do that. For instance, gradient-based methods, or methods that explore the effect of one parameter at a time (e.g., averaging the others) can be used as an alternative.



#### 4.2. Methodological innovation

Multi-layer modularity optimization is a valuable instrument to track the topological organization across instances of a multi-layer network. It exploits a resolution parameter that regulates nodes coupling across layers. Previous works pointed out how this backbone can be easily modified to address specific research questions (Zamani Esfahlani et al., 2021), and different efforts have been made in trying to properly model inter-layer coupling (e.g. (Amelio and Tagarelli, 2017; Di Plinio and Ebisch, 2022; Vaiana et al., 2019)). In this work we extended the classical multi-layer modularity maximization framework to address a long-standing question in neuroscience: what is the relationship between anatomical and functional modular organization and how this relationship is expressed across different individuals? Exploiting the flexibility of modularity optimization, we built a modularity matrix that contains multi-modal and multi-subject networks contemporaneously. The advantage of this method consists of having communities matched across layers, representing either individuals and type of connectivity. In this way, it allows a straightforward analysis of the modular structure: to get an estimate of whether communities are the same across connection modality and/or subjects, one can trivially compare community labels, without the need for additional heuristic. Previous studies already used the multi-layer framework (De Domenico, 2017; Vaiana and Muldoon, 2018) to track communities across subjects (Betzel et al., 2019), time (Baum et al., 2017; Betzel et al., 2017; Braun et al., 2015; Shine et al., 2016), frequency (Puxeddu et al., 2021b), learning paradigms (Bassett et al., 2011; Gerraty et al., 2018), tasks (Cole et al., 2014) clinical cohorts (He et al., 2018), or to model brain dynamics (Khambhati et al., 2018). Here, for the first time, thanks to the proposed extension, we could observe how the modular structure reorganizes across two distinct directions, that in our case were subjects and connection modality.

Ultimately, where is the novelty of our approach? Why it is useful? And why would we want a multi-modal, multi-subject model? The main novelty lies in that it allows for a straightforward comparison of the modular structure across multiple domains (in our case subjects and connectivity modality). Not only this is useful for discovery purposes (i.e. the investigation of structure-function relationship in the healthy brain), but also it could be applied in context with high clinical relevance, e.g. in clinical populations, where features of the relationships between structure and function can be used as biomarkers. An example could be a structure-function investigation in stroke patients, where anatomical connectivity is damaged and the way its relationship with functional connectivity mutates after the stroke event is crucial for rehabilitation purposes. Furthermore, one could also consider a multi-modal analysis across different tasks or cognitive states, where we might expect a variation in the structure-function coupling. Thus, this framework opens the door to new studies in which multiple co-occurrent factors can be taken into account in the analysis of the human brain topological organization. In general, more multi-layer approaches are needed to incorporate multiple channels of connectivity, to obtain a more thorough knowledge on the brain functioning.

Another important methodological aspect regards how we treated structural and functional matrices before incorporating them into the modularity matrix. In fact, it is good practice building multi-layer networks where layers are made of comparable weights, otherwise layers with higher weights may impact excessively the modularity optimization and thus the communities estimates. It is worth noticing that structural and functional networks are two distinct mathematical objects. A structural network is a sparse matrix with only positive weights, while a functional network is a full correlation matrix with both positive and negative weights. To overcome this difference, we converted structural matrices into structural *correlation* matrices. In this way, both functional and structural networks could be entered in the modularity matrix as similarity matrices, with weights falling in the same range, without running the risk of having one dragging the other in the community detection. This conversion also allowed us to use the same null

model in the modularity optimization, for both structural and functional layers.

Our transformation of anatomical networks also helped us in mitigating the differences between structural and functional networks in terms of inter-hemispheric connections. Notably, inter-hemispheric connections are difficult to reconstruct in structural networks, and are stronger in the functional networks, above all between homologous brain areas. A sensitivity analysis carried out running our model on a single hemisphere led to analogous results in terms of how the modes of SC-FC variability are embedded in the parameter space.

Finally, we want to point out that our computing the pairwise correlation between rows of structural matrices (to obtain correlation matrices) is similar to the computation of the matching index (Hilgetag et al., 2002), which captures the overlap of connection patterns for each pair of vertices. This index has been widely employed in the recent network neuroscience literature, for instance to study connection fingerprint (Sporns et al., 2007), build generative models (Betzel et al., 2016), or predict functional connectivity patterns from measures of network communication (Goñi et al., 2014). Another way to handle structural networks in the landscape of structure-function studies, is to transform them into communication matrices. Interestingly, in a recent work (Seguin et al., 2022), the authors showed that diffusion-based models help in approximating the functional modular organization better than routing models based on path efficiency.

#### 4.3. Technical considerations and limitations

In this study we focused on a specific kind on communities, i.e. modules, that are defined upon an assortative criterium (Girvan and Newman, 2002). It is well established that they well represent the brain networks organization (Sporns and Betzel, 2016), promoting states of segregation and integration (Fukushima et al., 2018), necessary for an efficient brain functioning (Wig, 2017). However, brain networks can also present different kind of organizations, based for example on core-periphery structure, disassortative communities or diffusion models (Betzel et al., 2018; Faskowitz and Sporns, 2020; Faskowitz et al., 2018; Newman, 2012). Recent studies started to explore different levels of brain networks organization (Faskowitz et al., 2020), with overlapping modules, so that future advancements could extend these efforts toward a multi-layer modeling. Furthermore, modularity maximization is not the only way, nor the best one, to find assortative communities in networks. However, as discussed in (Zamani Esfahlani et al., 2021), it is a useful and flexible tool to address specific questions of neuroscience, like the structure-function relationship, in a principled manner.

All the comparisons between structural and functional partitions, or among subjects, have been made through the Variation of Information and Entropy. We have chosen Variation of Information in line with previously mentioned studies based on modularity optimization, even if there are a number of indices that can be used alternatively (Gates et al., 2019). Moreover, we used Entropy because it provides both global and node-level scores of similarity between partitions, making it easy to localize changes of modular structure in the brain cortex.

Finally, a limitation of extended multi-layer optimization frameworks lies in their computational time. In fact, while in single-layer networks operations like modularity maximization are made on a modularity matrix whose dimension is given by the number of nodes, in multi-layer networks this same dimension is multiplied by the number of layers. Our proposed approach, by doubling the dimension of the multi-layer modularity matrix, requires even more memory and computational power and thus, does not scale well for extremely large datasets. Using a 100 nodes parcellation we optimized an already large modularity matrix, of dimension 24,600 ([123 subjects  $\times$  2 modalities  $\times$  100 nodes]). A single run of optimization of this dataset requires 7.3s on a laptop with an i7 processor and RAM 16GB. Using a 200 nodes parcellation, doubling the network dimension, requires 21s. This computational time must be multiplied by the number of combinations of resolution pa-



rameters (in our case we had  $[50 \times 50 \times 50]$  combinations). Small tricks can help us improve computational time. For instance, one can handle the modularity matrix as a function instead of as an object (Jutla et al., 2011), use parallel computing, or start the optimization by planting a seed partition (if there is a hypothesis a-priori). However, it is important to bear in mind that the computational cost does not scale linearly with the size of the modularity matrix, so even with these little tricks, a user should expect a heavy computational time and extensive memory usage.

#### 4.4. Future advances

There exists an increasing body of literature bringing attention to the influence of the brain network architecture on cognition and behavior (Bressler and Menon, 2010; McIntosh, 1999; Mišić and Sporns, 2016), and previous studies have shown that structure-function relationship and human behavior are also related (Medaglia et al., 2018). Moreover, structure-function relationship characterizes subjects individuality (Griffa et al., 2021). In this work, we propose as a supplemental investigation a preliminary analysis of how measures derived from four different cognitive assessments can be associated to the five modes of variability between structural and functional modular organization (section 9 of Supplementary Material). We observed that a relationship exists, and it is scale-dependent. Indeed, across the five principal components, most of the brain regions showed different patterns of correlation between SC-FC community entropy and IQ-based measures. Notably, the DMN is the subsystem whose patterns of correlations vary the least, maintaining always a positive correlation between IQ and its entropy across structure and function.

However, we only presented a proof-of-concept analyses to relate multi-scale partition information to cognitive assessments. To conclusively establish such relationships would likely require much larger sample sizes (Marek et al., 2022) and the application of additional tests and methodologies (Wu et al., 2021). For these reasons, we presented this part of the work without drawing strong conclusions (and we also invite the reader to make the same). Rather, we illustrated brain-wide patterns at different scales, proving that our proposed methodology, by preserving single-subject information while allowing the exploration along a third dimension, could be useful in future studies to properly investigate brain-behavior associations. Furthermore, in these studies, the magnitude of the correlation between network topology and behavioral indices can be used to restrict the space of investigation to only those parameter combinations that lead to the most fruitful associations. This could be an alternative to the PCA analysis that we carried out.

Another direction for further investigations, could be analyzing how the relationship between structural and functional topology relates to attributes of the modular structure. For instance, we made a preliminary analysis in which we linked measures of segregation and integration to the cross-modality entropy (Supplementary Material, section 8). What we found is that a relationship between all these measures exists, and subjects with highly segregated functional networks tend to have a weaker coupling between structural and functional topology. Again, we want to emphasize that these relationships can be investigated only with our extended model, that allows for a simultaneous tracking of inter-subject and inter-modality features.

Finally, we want to highlight that our focus was on a restricted category of participants, that is healthy adults. Future works could apply the proposed methods to clinical cohorts, to investigate if and how the relationship between structure and function changes with diseases. To do that, there exist different possible strategies. For instance, one could include structural and functional networks from patients and controls in the same structure-function modularity matrix, or build two modularity matrices, one for each category. Then, the next steps would be including a local entropy analysis to see how structural and functional topological organization varies in different brain regions within and between the two cohorts. In this case, entropy profiles could be used as prognostic

indices, or to predict clinical outcomes, if clinical scales are available. These indices could be validated through different permutation-based null models, e.g., by randomly assigning participants to cohorts, randomizing node order so that node  $i$  is connected to  $j \neq i$  across layers, or by randomly coupling structural and functional matrices from different subjects. Using these approaches, we can generate null entropy measures that can subsequently be compared against the observed entropy scores.

Ultimately, the framework we propose can be used in lifespan studies or could be further extended by including time-varying or task-specific functional matrices, instead of single resting-state ones. This would allow linking different dynamic states to their underlying anatomical substrate.

## 5. Conclusion

In conclusion, we developed a novel multi-layer framework able to incorporate multiple modes of connectivity, so that we could quantify how much the network modular structure varies across connection modality and subjects simultaneously. We investigated the relationship between structural and functional brain networks modular organization, and how it is shaped across subjects and at different spatial scales. While confirming previous findings on specific brain areas, our results provide also evidence that these relationships are recapitulated by scale-dependent modes of variability. Overall, this work not only increases the state-of-the-art methods and knowledge about structure-function relationship, but also enables new analysis that can be done to comprehensively map the human brain networks organization across multiple domains.

### Code availability

MATLAB code to build the multi-modal and multi-subject network and run the extended modularity optimization is available at [https://github.com/mariagraziaP/multimodal\\_multisubject\\_modularity](https://github.com/mariagraziaP/multimodal_multisubject_modularity).

### Credit authorship contribution statement

**Maria Grazia Puxeddu:** Conceptualization, Formal analysis, Methodology, Writing – original draft, Writing – review & editing. **Joshua Faskowitz:** Data curation, Writing – review & editing. **Olaf Sporns:** Writing – review & editing. **Laura Astolfi:** Writing – review & editing. **Richard F. Betzel:** Conceptualization, Methodology, Writing – original draft, Writing – review & editing, Supervision.

## References

- Adachi, Y., Osada, T., Sporns, O., Watanabe, T., Matsui, T., Miyamoto, K., Miyashita, Y., 2012. Functional connectivity between anatomically unconnected areas is shaped by collective network-level effects in the macaque cortex. *Cereb. Cortex* 22 (7), 1586–1592. doi:10.1093/cercor/bhr234.
- Alexander-Bloch, A.F., Shou, H., Liu, S., Satterthwaite, T.D., Glahn, D.C., Shinohara, R.T., Vandekar, S.N., Raznahan, A., 2018. On testing for spatial correspondence between maps of human brain structure and function. *Neuroimage* 178, 540–551. doi:10.1016/j.neuroimage.2018.05.070.
- Amelio, A., Tagarelli, A., 2017. Revisiting Resolution and Inter-Layer Coupling Factors in Modularity for Multilayer Networks. In: Proceedings of the 2017 IEEE/ACM International Conference on Advances in Social Networks Analysis and Mining 2017. Association for Computing Machinery, New York, NY, USA, pp. 266–273. doi:10.1145/3110025.3110051.
- Amico, E., Goñi, J., 2018. Mapping hybrid functional-structural connectivity traits in the human connectome. *Network Neurosci.* 2 (3), 306–322. doi:10.1162/netn\_a\_00049. Publisher: MIT Press
- Bansal, K., Nakuci, J., Muldoon, S.F., 2018. Personalized brain network models for assessing structure–function relationships. *Curr. Opin. Neurobiol.* 52, 42–47.
- Bassett, D.S., Sporns, O., 2017. Network neuroscience. *Nat. Neurosci.* 20 (3), 353–364. doi:10.1038/nn.4502.
- Bassett, D.S., Wymbs, N.F., Porter, M.A., Mucha, P.J., Carlson, J.M., Grafton, S.T., 2011. Dynamic reconfiguration of human brain networks during learning. *Proc. Natl. Acad. Sci.* 108 (18), 7641–7646. doi:10.1073/pnas.1018985108.
- Batista-García-Ramó, K., Fernández-Verdecia, C.I., 2018. What we know about the brain structure function relationship. *Behav. Sci.* 8 (4), 39. doi:10.3390/bs8040039. Number: 4 Publisher: Multidisciplinary Digital Publishing Institute

- Baum, G.L., Ciric, R., Roalf, D.R., Betzel, R.F., Moore, T.M., Shinohara, R.T., Kahn, A.E., Vandekar, S.N., Rupert, P.E., Quarmley, M., Cook, P.A., Elliott, M.A., Ruparel, K., Gur, R.E., Gur, R.C., Bassett, D.S., Satterthwaite, T.D., 2017. Modular segregation of structural brain networks supports the development of executive function in youth. *Curr. Biol.* 27 (11), 1561–1572.e8. doi:10.1016/j.cub.2017.04.051.
- Bazzi, M., Porter, M.A., Williams, S., McDonald, M., Fenn, D.J., Howison, S.D., 2016. Community detection in temporal multilayer networks, with an application to correlation networks. *Multiscale Model. Simulat.* 14 (1), 1–41. doi:10.1137/15M1009615. Publisher: Society for Industrial and Applied Mathematics
- Betzel, R.F., Avena-Koenigsberger, A., Go, J., He, Y., de Reus, M.A., Griffa, A., Vértés, P.E., Mišić, B., Thiran, J.-P., Hagmann, P., van den Heuvel, M., Zuo, X.-N., Bullmore, E.T., Sporns, O., 2016. Generative models of the human connectome. *Neuroimage* 124, 1054–1064. doi:10.1016/j.neuroimage.2015.09.041.
- Betzel, R.F., Bassett, D.S., 2017. Multi-scale brain networks. *Neuroimage* 160, 73–83. doi:10.1016/j.neuroimage.2016.11.006.
- Betzel, R.F., Bertolero, M.A., Gordon, E.M., Gratton, C., Dosenbach, N.U.F., Bassett, D.S., 2019. The community structure of functional brain networks exhibits scale-specific patterns of inter- and intra-subject variability. *Neuroimage* doi:10.1016/j.neuroimage.2019.07.003.
- Betzel, R.F., Griffa, A., Avena-Koenigsberger, A., Goñi, J., Thiran, J.-P., Hagmann, P., Sporns, O., 2013. Multi-scale community organization of the human structural connectome and its relationship with resting-state functional connectivity. *Netw. Sci.* 1 (3), 353–373. doi:10.1017/nws.2013.19.
- Betzel, R.F., Medaglia, J.D., Bassett, D.S., 2018. Diversity of meso-scale architecture in human and non-human connectomes. *Nat. Commun.* 9 (1), 1–14. doi:10.1038/s41467-017-02681-z.
- Betzel, R.F., Satterthwaite, T.D., Gold, J.I., Bassett, D.S., 2017. Positive affect, surprise, and fatigue are correlates of network flexibility. *Sci. Rep.* 7 (1), 1–10. doi:10.1038/s41598-017-00425-z.
- Braun, U., Schfer, A., Walter, H., Erk, S., Romanczuk-Seiferth, N., Haddad, L., Schweiger, J.I., Grimm, O., Heinz, A., Tost, H., Meyer-Lindenberg, A., Bassett, D.S., 2015. Dynamic reconfiguration of frontal brain networks during executive cognition in humans. *Proc. Natl. Acad. Sci.* 112 (37), 11678–11683. doi:10.1073/pnas.1422487112.
- Breakspear, M., 2017. Dynamic models of large-scale brain activity. *Nat. Neurosci.* 20 (3), 340–352. doi:10.1038/nn.4497.
- Bressler, S.L., Menon, V., 2010. Large-scale brain networks in cognition: emerging methods and principles. *Trends Cogn. Sci. (Regul. Ed.)* 14 (6), 277–290. doi:10.1016/j.tics.2010.04.004. Publisher: Elsevier
- Buckner, R.L., DiNicola, L.M., 2019. The brain's default network: updated anatomy, physiology and evolving insights. *Nat. Rev. Neurosci.* 20 (10), 593–608. doi:10.1038/s41583-019-0212-7.
- Cole, M.W., Bassett, D.S., Power, J.D., Braver, T.S., Petersen, S.E., 2014. Intrinsic and task-evoked network architectures of the human brain. *Neuron* 83 (1), 238–251. doi:10.1016/j.neuron.2014.05.014.
- Crofts, J.J., Higham, D.J., 2009. A weighted communicability measure applied to complex brain networks. *J. R. Soc. Interface* 6 (33), 411–414. doi:10.1098/rsif.2008.0484.
- De Domenico, M., 2017. Multilayer modeling and analysis of human brain networks. *Gigascience* 6 (5). doi:10.1093/gigascience/gix004.
- De Domenico, M., Sasaki, S., Arenas, A., 2016. Mapping multiplex hubs in human functional brain networks. *Front. Neurosci.* 10.
- Deco, G., Jirsa, V., McIntosh, A.R., Sporns, O., Ktter, R., 2009. Key role of coupling, delay, and noise in resting brain fluctuations. *Proc. Natl. Acad. Sci.* 106 (25), 10302–10307. doi:10.1073/pnas.0901831106.
- Di Plinio, S., Ebisch, S.J.H., 2022. Probabilistically weighted multilayer networks disclose the link between default mode network instability and psychosis-like experiences in healthy adults. *Neuroimage* 257, 119291. doi:10.1016/j.neuroimage.2022.119291.
- Diez, I., Bonifazi, P., Escudero, I., Mateos, B., Muoz, M.A., Stramaglia, S., Cortes, J.M., 2015. A novel brain partition highlights the modular skeleton shared by structure and function. *Sci. Rep.* 5 (1), 10532. doi:10.1038/srep10532. Number: 1 Publisher: Nature Publishing Group
- Faskowitz, J., Esfahani, F.Z., Jo, Y., Sporns, O., Betzel, R.F., 2020. Edge-centric functional network representations of human cerebral cortex reveal overlapping system-level architecture. *Nat. Neurosci.* 1–11. doi:10.1038/s41593-020-00719-y. Publisher: Nature Publishing Group
- Faskowitz, J., Sporns, O., 2020. Mapping the community structure of the rat cerebral cortex with weighted stochastic block modeling. *Brain Struct. Funct.* 225 (1), 71–84.
- Faskowitz, J., Yan, X., Zuo, X.-N., Sporns, O., 2018. Weighted stochastic block models of the human connectome across the life span. *Sci. Rep.* 8 (1), 12997. doi:10.1038/s41598-018-31202-1.
- Finn, E.S., Shen, X., Scheinost, D., Rosenberg, M.D., Huang, J., Chun, M.M., Papademetris, X., Constable, R.T., 2015. Functional connectome fingerprinting: identifying individuals using patterns of brain connectivity. *Nat. Neurosci.* 18 (11), 1664–1671. doi:10.1038/nn.4135.
- Fortunato, S., 2010. Community detection in graphs. *Phys. Rep.* 486 (3), 75–174. doi:10.1016/j.physrep.2009.11.002.
- Fox, M.D., Snyder, A.Z., Vincent, J.L., Corbetta, M., Essen, D.C.V., Raichle, M.E., 2005. The human brain is intrinsically organized into dynamic, anticorrelated functional networks. *Proc. Natl. Acad. Sci.* 102 (27), 9673–9678. doi:10.1073/pnas.0504136102.
- Friston, K.J., 1994. Functional and effective connectivity in neuroimaging: a synthesis. *Hum. Brain Mapp.* 2 (1–2), 56–78. doi:10.1002/hbm.460020107.
- Friston, K.J., 2011. Functional and effective connectivity: a review. *Brain Connect.* 1 (1), 13–36. doi:10.1089/brain.2011.0008.
- Fukushima, M., Betzel, R.F., He, Y., van den Heuvel, M.P., Zuo, X.-N., Sporns, O., 2018. Structure-function relationships during segregated and integrated network states of human brain functional connectivity. *Brain Structure and Function* 223 (3), 1091–1106. doi:10.1007/s00429-017-1539-3.
- Gates, A.J., Wood, I.B., Hetrick, W.P., Ahn, Y.-Y., 2019. Element-centric clustering comparison unifies overlaps and hierarchy. *Sci. Rep.* 9 (1), 8574. doi:10.1038/s41598-019-44892-y. a Ce.license.type: cc-by Cg.type: Nature Research Journals Number: 1 Primary\_atype: Research Publisher: Nature Publishing Group Subject term: Complex networks;Data mining;Modularity;Network models Subject term\_id: complex-networks;data-mining;modularity;network-models
- Gerraty, R.T., Davidow, J.Y., Foerster, K., Galvan, A., Bassett, D.S., Shohamy, D., 2018. Dynamic flexibility in striatal-cortical circuits supports reinforcement learning. *J. Neurosci.* 38 (10), 2442–2453. doi:10.1523/JNEUROSCI.2084-17.2018.
- Girvan, M., Newman, M.E.J., 2002. Community structure in social and biological networks. *Proc. Natl. Acad. Sci. U.S.A.* 99 (12), 7821–7826. doi:10.1073/pnas.122653799.
- Glasser, M.F., Sotiropoulos, S.N., Wilson, J.A., Coalson, T.S., Fischl, B., Andersson, J.L., Xu, J., Jbabdi, S., Webster, M., Polimeni, J.R., Essen, D.C.V., Jenkinson, M., 2013. The minimal preprocessing pipelines for the human connectome project. *Neuroimage* 80, 105–124. doi:10.1016/j.neuroimage.2013.04.127.
- Goñi, J., Heuvel, v.d.M.P., Avena-Koenigsberger, A., Mendizabal, d.N.V., Betzel, R.F., Griffa, A., Hagmann, P., Corominas-Murtra, B., Thiran, J.-P., Sporns, O., 2014. Resting-brain functional connectivity predicted by analytic measures of network communication. *Proc. Natl. Acad. Sci.* 111 (2), 833–838. doi:10.1073/pnas.1315529111.
- Gordon, E.M., Laumann, T.O., Gilmore, A.W., Newbold, D.J., Greene, D.J., Berg, J.J., Ortega, M., Hoyt-Drazen, C., Gratton, C., Sun, H., Hampton, J.M., Coalson, R.S., Nguyen, A.L., McDermott, K.B., Shimony, J.S., Snyder, A.Z., Schlaggar, B.L., Petersen, S.E., Nelson, S.M., Dosenbach, N.U.F., 2017. Precision functional mapping of individual human brains. *Neuron* 95 (4), 791–807.e7. doi:10.1016/j.neuron.2017.07.011.
- Griffa, A., Amico, E., Liégeois, R., Ville, D.V.D., Preti, M.G., 2021. Structure-function interplay as signature for brain decoding and fingerprinting. *bioRxiv*, 2021.04.19.440314 doi:10.1101/2021.04.19.440314. Publisher: Cold Spring Harbor Laboratory Section: New Results
- Hagmann, P., Cammoun, L., Gigandet, X., Meuli, R., Honey, C.J., Wedeen, V.J., Sporns, O., 2008. Mapping the structural core of human cerebral cortex. *PLoS Biol.* 6 (7), e159. doi:10.1371/journal.pbio.0060159.
- He, Y., Lim, S., Fortunato, S., Sporns, O., Zhang, L., Qiu, J., Xie, P., Zuo, X.-N., 2018. Reconfiguration of cortical networks in MDD uncovered by multiscale community detection with fmri. *Cereb. Cortex* 28 (4), 1383–1395. doi:10.1093/cercor/bhx335.
- Hilgetag, C.C., Ktter, R., Stephan, K.E., Sporns, O., 2002. Computational Methods for the Analysis of Brain Connectivity. In: G.A. Ascoli (Ed.), *Computational Neuroanatomy Principles and Methods*. Humana Press, Totowa, NJ, pp. 295–335. doi:10.1007/978-1-59259-275-3\_14.
- Honey, C.J., Ktter, R., Breakspear, M., Sporns, O., 2007. Network structure of cerebral cortex shapes functional connectivity on multiple time scales. *Proc. Natl. Acad. Sci.* 104 (24), 10240–10245. doi:10.1073/pnas.0701519104.
- Honey, C.J., Thivierge, J.-P., Sporns, O., 2010. Can structure predict function in the human brain? *Neuroimage* 52 (3), 766–776. doi:10.1016/j.neuroimage.2010.01.071.
- Jutla, I.S., Jeub, L.G.S., Mucha, P.J., 2011. A generalized louvain method for community detection implemented in Matlab. <http://networks.amath.unc.edu/GenLouvain>
- Khambhati, A.N., Sizemore, A.E., Betzel, R.F., Bassett, D.S., 2018. Modeling and interpreting mesoscale network dynamics. *Neuroimage* 180, 337–349. doi:10.1016/j.neuroimage.2017.06.029.
- Laumann, T.O., Gordon, E.M., Adeyemo, B., Snyder, A.Z., Joo, S.J., Chen, M.-Y., Gilmore, A.W., McDermott, K.B., Nelson, S.M., Dosenbach, N.U.F., Schlaggar, B.L., Mumford, J.A., Poldrack, R.A., Petersen, S.E., 2015. Functional system and areal organization of a highly sampled individual human brain. *Neuron* 87 (3), 657–670. doi:10.1016/j.neuron.2015.06.037.
- Marek, S., Tervo-Clemmens, B., Calabro, F.J., Montez, D.F., Kay, B.P., Hatoum, A.S., Donohue, M.R., Foran, W., Miller, R.L., Hendrickson, T.J., Malone, S.M., Kandal, S., Feczko, E., Miranda-Dominguez, O., Graham, A.M., Earl, E.A., Perrone, A.J., Cordova, M., Doyle, O., Moore, L.A., Conan, G.M., Uriarte, J., Snider, K., Lynch, B.J., Wilgenbusch, J.C., Pengo, T., Tam, A., Chen, J., Newbold, D.J., Zheng, A., Seider, N.A., Van, A.N., Metoki, A., Chauvin, R.J., Laumann, T.O., Greene, D.J., Petersen, S.E., Garavan, H., Thompson, W.K., Nichols, T.E., Yeo, B.T.T., Barch, D.M., Luna, B., Fair, D.A., Dosenbach, N.U.F., 2022. Reproducible brain-wide association studies require thousands of individuals. *Nature* 603 (7902), 654–660. doi:10.1038/s41586-022-04492-9. Number: 7902 Publisher: Nature Publishing Group
- McIntosh, A.R., 1999. Mapping cognition to the brain through neural interactions. *Memory* 7 (5–6), 523–548. doi:10.1080/096582199387733. Place: United Kingdom Publisher: Taylor & Francis
- McIntosh, A.R., 2000. Towards a network theory of cognition. *Neural Netw.* 13 (8), 861–870. doi:10.1016/S0893-6080(00)00059-9.
- Medaglia, J.D., Huang, W., Karuza, E.A., Kelkar, A., Thompson-Schill, S.L., Ribeiro, A., Bassett, D.S., 2018. Functional alignment with anatomical networks is associated with cognitive flexibility. *Nat. Hum. Behav.* 2 (2), 156–164. doi:10.1038/s41562-017-0260-9.
- Medaglia, J.D., Lynall, M.-E., Bassett, D.S., 2015. Cognitive network neuroscience. *J. Cogn. Neurosci.* 27 (8), 1471–1491. doi:10.1162/jocn.a.00810.
- Meil, M., 2007. Comparing clusterings an information based distance. *J. Multivar. Anal.* 98 (5), 873–895. doi:10.1016/j.jmva.2006.11.013.
- Messé, A., Rudrauf, D., Giron, A., Marrelec, G., 2015. Predicting functional connectivity from structural connectivity via computational models using MRI: an extensive comparison study. *Neuroimage* 111, 65–75. doi:10.1016/j.neuroimage.2015.02.001.
- Meunier, D., Lambiotte, R., Bullmore, E.T., 2010. Modular and hierarchically modular organization of brain networks. *Front. Neurosci.* 4. doi:10.3389/fnins.2010.00200.

- Meunier, D., Lambiotte, R., Fornito, A., Ersche, K., Bullmore, E.T., 2009. Hierarchical modularity in human brain functional networks. *Front. Neuroinform.* 3. doi:[10.3389/neuro.11.037.2009](https://doi.org/10.3389/neuro.11.037.2009).
- Mišić, B., Betzel, R.F., de Reus, M.A., van den Heuvel, M.P., Berman, M.G., McIntosh, A.R., Sporns, O., 2016. Network-level structure-function relationships in human neocortex. *Cereb. Cortex* 26 (7), 3285–3296. doi:[10.1093/cercor/bhw089](https://doi.org/10.1093/cercor/bhw089).
- Mišić, B., Sporns, O., 2016. From regions to connections and networks: new bridges between brain and behavior. *Curr. Opin. Neurobiol.* 40, 1–7. doi:[10.1016/j.conb.2016.05.003](https://doi.org/10.1016/j.conb.2016.05.003).
- Mucha, P.J., Richardson, T., Macon, K., Porter, M.A., Onnela, J.-P., 2010. Community structure in time-dependent, multiscale, and multiplex networks. *Science* 328 (5980), 876–878. doi:[10.1126/science.1184819](https://doi.org/10.1126/science.1184819).
- Newman, M.E.J., 2012. Communities, modules and large-scale structure in networks. *Nat. Phys.* 8 (1), 25–31. doi:[10.1038/nphys2162](https://doi.org/10.1038/nphys2162).
- Newman, M.E.J., Girvan, M., 2004. Finding and evaluating community structure in networks. *Phys. Rev. E* 69 (2). doi:[10.1103/PhysRevE.69.026113](https://doi.org/10.1103/PhysRevE.69.026113).
- Nooner, K.B., Colcombe, S., Tobe, R., Mennes, M., Benedict, M., Moreno, A., Panek, L., Brown, S., Zavitz, S., Li, Q., Sikka, S., Gutman, D., Bangaru, S., Schlachter, R.T., Kamiel, S., Anwar, A., Hinz, C., Kaplan, M., Rachlin, A., Adelsberg, S., Cheung, B., Khanuja, R., Yan, C., Craddock, C., Calhoun, V., Courtney, W., King, M., Wood, D., Cox, C., Kelly, C., DiMartino, A., Petkova, E., Reiss, P., Duan, N., Thompsen, D., Biswal, B., Coffey, B., Hoptman, M., Javitt, D.C., Pomara, N., Sidtis, J., Koplewicz, H., Castellanos, F.X., Leventhal, B., Milham, M., 2012. The NKI-rockland sample: a model for accelerating the pace of discovery science in psychiatry. *Front. Neurosci.* 6. doi:[10.3389/fnins.2012.00152](https://doi.org/10.3389/fnins.2012.00152).
- Paquola, C., Wael, R.V.D., Wagstyl, K., Bethlehem, R.A.I., Hong, S.-J., Seidlitz, J., Bullmore, E.T., Evans, A.C., Misić, B., Margulies, D.S., Smallwood, J., Bernhardt, B.C., 2019. Microstructural and functional gradients are increasingly dissociated in transmodal cortices. *PLoS Biol.* 17 (5), e3000284. doi:[10.1371/journal.pbio.3000284](https://doi.org/10.1371/journal.pbio.3000284). Publisher: Public Library of Science.
- Park, H.-J., Friston, K., 2013. Structural and functional brain networks: from connections to cognition. *Science* 342 (6158), 1238411. doi:[10.1126/science.1238411](https://doi.org/10.1126/science.1238411).
- Preti, M.G., Van De Ville, D., 2019. Decoupling of brain function from structure reveals regional behavioral specialization in humans. *Nat. Commun.* 10 (1), 4747. doi:[10.1038/s41467-019-12765-7](https://doi.org/10.1038/s41467-019-12765-7).
- Puxeddu, M., Petti, M., Mattia, D., Astolfi, L., 2019. The Optimal Setting for Multilayer Modularity Optimization in Multilayer Brain Networks\*. In: 2019 41st Annual International Conference of the IEEE Engineering in Medicine and Biology Society (EMBC), pp. 624–627. doi:[10.1109/EMBC.2019.8856674](https://doi.org/10.1109/EMBC.2019.8856674). ISSN: 1558-4615.
- Puxeddu, M.G., Faskowitz, J., Betzel, R.F., Petti, M., Astolfi, L., Sporns, O., 2020. The modular organization of brain cortical connectivity across the human lifespan. *Neuroimage* 218, 116974. doi:[10.1016/j.neuroimage.2020.116974](https://doi.org/10.1016/j.neuroimage.2020.116974).
- Puxeddu, M.G., Petti, M., Astolfi, L., 2021. A comprehensive analysis of multilayer community detection algorithms for application to EEG-based brain networks. *Front. Syst. Neurosci.* 15. doi:[10.3389/fnsys.2021.624183](https://doi.org/10.3389/fnsys.2021.624183). Publisher: Frontiers.
- Puxeddu, M.G., Petti, M., Astolfi, L., 2021. Multi-layer analysis of multi-frequency brain networks as a new tool to study EEG topological organization. In: 2021 43rd Annual International Conference of the IEEE Engineering in Medicine Biology Society (EMBC), pp. 924–927. doi:[10.1109/EMBC46164.2021.9630173](https://doi.org/10.1109/EMBC46164.2021.9630173). ISSN: 2694-0604.
- Rosenthal, G., Sporns, O., Avidan, G., 2017. Stimulus dependent dynamic reorganization of the human face processing network. *Cereb. Cortex* 27 (10), 4823–4834. doi:[10.1093/cercor/bhw279](https://doi.org/10.1093/cercor/bhw279).
- Sarwar, T., Tian, Y., Yeo, B.T.T., Ramamohanarao, K., Zalesky, A., 2021. Structure-function coupling in the human connectome: a machine learning approach. *Neuroimage* 226, 117609. doi:[10.1016/j.neuroimage.2020.117609](https://doi.org/10.1016/j.neuroimage.2020.117609).
- Thiebaut de Schotten, M., Foulon, C., Nachev, P., 2020. Brain disconnections link structural connectivity with function and behaviour. *Nat. Commun.* 11 (1), 5094. doi:[10.1038/s41467-020-18920-9](https://doi.org/10.1038/s41467-020-18920-9). Number: 1 Publisher: Nature Publishing Group.
- Seguin, C., Mansour, L. S., Sporns, O., Zalesky, A., Calamante, F., 2022. Network communication models narrow the gap between the modular organization of structural and functional brain networks. *Neuroimage* 119323. doi:[10.1016/j.neuroimage.2022.119323](https://doi.org/10.1016/j.neuroimage.2022.119323).
- Shine, J.M., Bisset, P.G., Bell, P.T., Koyejo, O., Balsters, J.H., Gorgolewski, K.J., Moodie, C.A., Poldrack, R.A., 2016. The dynamics of functional brain networks: integrated network states during cognitive task performance. *Neuron* 92 (2), 544–554. doi:[10.1016/j.neuron.2016.09.018](https://doi.org/10.1016/j.neuron.2016.09.018).
- Sporns, O., 2011. The human connectome: a complex network. *Ann. N. Y. Acad. Sci.* 1224, 109–125. doi:[10.1111/j.1749-6632.2010.05888.x](https://doi.org/10.1111/j.1749-6632.2010.05888.x).
- Sporns, O., Betzel, R.F., 2016. Modular brain networks. *Annu. Rev. Psychol.* 67, 613–640. doi:[10.1146/annurev-psych-122414-033634](https://doi.org/10.1146/annurev-psych-122414-033634).
- Sporns, O., Honey, C.J., Kter, R., 2007. Identification and classification of hubs in brain networks. *PLoS ONE* 2 (10), e1049. doi:[10.1371/journal.pone.0001049](https://doi.org/10.1371/journal.pone.0001049). Publisher: Public Library of Science.
- Stam, C.J., van Straaten, E.C.W., Van Dellen, E., Tewarie, P., Gong, G., Hillebrand, A., Meier, J., Van Mieghem, P., 2016. The relation between structural and functional connectivity patterns in complex brain networks. *Int. J. Psychophysiol.* 103, 149–160. doi:[10.1016/j.ijpsycho.2015.02.011](https://doi.org/10.1016/j.ijpsycho.2015.02.011).
- Suárez, L.E., Markello, R.D., Betzel, R.F., Misić, B., 2020. Linking structure and function in macroscale brain networks. *Trends Cogn. Sci. (Regul. Ed.)* 24 (4), 302–315. doi:[10.1016/j.tics.2020.01.008](https://doi.org/10.1016/j.tics.2020.01.008).
- Thomas Yeo, B.T., Krienen, F.M., Sepulcre, J., Sabuncu, M.R., Lashkari, D., Hollinshead, M., Roffman, J.L., Smoller, J.W., Zlei, L., Polimeni, J.R., Fischl, B., Liu, H., Buckner, R.L., 2011. The organization of the human cerebral cortex estimated by intrinsic functional connectivity. *J. Neurophysiol.* 106 (3), 1125–1165. doi:[10.1152/jn.00338.2011](https://doi.org/10.1152/jn.00338.2011).
- Traag, V.A., Van Dooren, P., Nesterov, Y., 2011. Narrow scope for resolution-limit-free community detection. *Phys. Rev. E* 84 (1), 016114. doi:[10.1103/PhysRevE.84.016114](https://doi.org/10.1103/PhysRevE.84.016114). Publisher: American Physical Society.
- Vaiana, M., Goldberg, E.M., Muldoon, S.F., 2019. Optimizing state change detection in functional temporal networks through dynamic community detection. *J. Complex. Netw.* 7 (4), 529–553. doi:[10.1093/comnet/cny030](https://doi.org/10.1093/comnet/cny030).
- Vaiana, M., Muldoon, S.F., 2018. Multilayer brain networks. *J. Nonlinear Sci.* doi:[10.1007/s00332-017-9436-8](https://doi.org/10.1007/s00332-017-9436-8).
- Van Essen, D.C., Smith, S.M., Barch, D.M., Behrens, T.E.J., Yacoub, E., Ugurbil, K., 2013. The WU-minn human connectome project: an overview. *Neuroimage* 80, 62–79. doi:[10.1016/j.neuroimage.2013.05.041](https://doi.org/10.1016/j.neuroimage.2013.05.041).
- Vatansever, D., Menon, D.K., Manktelow, A.E., Sahakian, B.J., Stamatakis, E.A., 2015. Default mode dynamics for global functional integration. *J. Neurosci.* 35 (46), 15254–15262. doi:[10.1523/JNEUROSCI.2135-15.2015](https://doi.org/10.1523/JNEUROSCI.2135-15.2015).
- Vázquez-Rodríguez, B., Suárez, L.E., Markello, R.D., Shafiei, G., Paquola, C., Hagmann, P., Heuvel, v.d.M.P., Bernhardt, B.C., Spreng, R.N., Misić, B., 2019. Gradients of structure-function tethering across neocortex. *Proc. Natl. Acad. Sci.* 116 (42), 21219–21227. doi:[10.1073/pnas.1903403116](https://doi.org/10.1073/pnas.1903403116).
- Wig, G.S., 2017. Segregated systems of human brain networks. *Trends Cogn. Sci. (Regul. Ed.)* 21 (12), 981–996. doi:[10.1016/j.tics.2017.09.006](https://doi.org/10.1016/j.tics.2017.09.006).
- Wu, J., Eickhoff, S.B., Hoffstaedter, F., Patil, K.R., Schwender, H., Yeo, B.T.T., Genon, S., 2021. A connectivity-based psychometric prediction framework for brain-behavior relationship studies. *Cereb. Cortex* (bhab044) doi:[10.1093/cercor/bhab044](https://doi.org/10.1093/cercor/bhab044).
- Zamani Esfahlani, F., Faskowitz, J., Slack, J., Mišić, B., Betzel, R.F., 2022. Local structure-function relationships in human brain networks across the lifespan. *Nat. Commun.* 13 (1), 2053. doi:[10.1038/s41467-022-29770-y](https://doi.org/10.1038/s41467-022-29770-y). Number: 1 Publisher: Nature Publishing Group.
- Zamani Esfahlani, F., Jo, Y., Puxeddu, M.G., Merritt, H., Tanner, J.C., Greenwell, S., Patel, R., Faskowitz, J., Betzel, R.F., 2021. Modularity maximization as a flexible and generic framework for brain network exploratory analysis. *Neuroimage* 244, 118607. doi:[10.1016/j.neuroimage.2021.118607](https://doi.org/10.1016/j.neuroimage.2021.118607).
- Zhang, J., Cheng, W., Liu, Z., Zhang, K., Lei, X., Yao, Y., Becker, B., Liu, Y., Kendrick, K.M., Lu, G., Feng, J., 2016. Neural, electrophysiological and anatomical basis of brain-network variability and its characteristic changes in mental disorders. *Brain: A Journal of Neurology* 139 (Pt 8), 2307–2321. doi:[10.1093/brain/aww143](https://doi.org/10.1093/brain/aww143).